



HAL
open science

Niche partitioning and plastisphere core microbiomes in the two most plastic polluted zones of the world ocean

Justine Jacquin, Marko Budinich, Samuel Chaffron, Valérie Barbe, Fabien Lombard, Maria-Luiza Pedrotti, Gabriel Gorsky, Alexandra ter Halle, Stéphane Bruzaud, Mikaël Kedzierski, et al.

► To cite this version:

Justine Jacquin, Marko Budinich, Samuel Chaffron, Valérie Barbe, Fabien Lombard, et al.. Niche partitioning and plastisphere core microbiomes in the two most plastic polluted zones of the world ocean. *Environmental Science and Pollution Research*, 2024, 31 (28), pp.41118-41136. 10.1007/s11356-024-33847-0 . hal-04625794

HAL Id: hal-04625794

<https://hal.science/hal-04625794>

Submitted on 26 Jun 2024

HAL is a multi-disciplinary open access archive for the deposit and dissemination of scientific research documents, whether they are published or not. The documents may come from teaching and research institutions in France or abroad, or from public or private research centers.

L'archive ouverte pluridisciplinaire **HAL**, est destinée au dépôt et à la diffusion de documents scientifiques de niveau recherche, publiés ou non, émanant des établissements d'enseignement et de recherche français ou étrangers, des laboratoires publics ou privés.

1 **Title:** Niche partitioning and plastisphere core microbiomes in the two most plastic polluted
2 zones of the world Ocean

3

4 **List of authors:** Justine Jacquin¹[⊙], Marko Budinich^{2,3}[⊙], Samuel Chaffron^{3,4}, Valérie Barbe⁵,
5 Fabien Lombard⁶, Maria-Luiza Pedrotti ⁶, Gabriel Gorsky⁶, Alexandra ter Halle⁷, Stéphane
6 Bruzaud⁸, Mikaël Kedzierski⁸, Jean-François Ghiglione^{1,3*}

7

8 [⊙] Shared co-first authorship

9

10 **(*) Corresponding author:** Jean-François Ghiglione, Laboratoire d'Océanographie
11 Microbienne, 1 Avenue Fabre, F-66650 Banyuls sur mer, France, Email : ghiglione@obs-
12 banyuls.fr

13

14 **Affiliations :**

15 1. CNRS, Sorbonne Université, UMR 7621, Laboratoire d'Océanographie Microbienne
16 (LOMIC), Banyuls sur mer, France

17 2. CNRS, Sorbonne Université, Laboratoire Adaptation et Diversité en Milieu Marin, Station
18 Biologique de Roscoff, Roscoff, France

19 3. Research Federation for the Study of Global Ocean Systems Ecology and Evolution,
20 FR2022/Tara Oceans GOSEE, Paris, France.

21 4. Nantes Université, École Centrale Nantes, CNRS, LS2N, UMR 6004, F-44000 Nantes,
22 France.

23 5. Génomique Métabolique, Genoscope, Institut François Jacob, CEA, CNRS, Univ Evry,
24 Université Paris-Saclay, Evry, France

25 6. Sorbonne Université, CNRS UMR 7076, Laboratoire d'Océanographie de Villefranche,
26 Villefranche sur mer, France.

27 7. CNRS, Université de Toulouse III-Paul Sabatier, UMR 5623, Laboratoire SOFMAT,
28 Toulouse, France

29 8. Institut de Recherche Dupuy de Lôme (IRDL), Université de Bretagne-Sud, UMR CNRS
30 6027, Lorient, France

31

32

33 **Keywords:** Plastic debris; plastisphere; core microbiome; microbial ecotoxicology

34

35 **Abstract:**

36 Plastics are offering a new niche for microorganisms colonizing their surface, the so-called
37 'plastisphere', in which diversity and community structure remain to be characterized and
38 compared across ocean pelagic regions. Here we compared the bacterial diversity of
39 microorganisms living on plastic marine debris (PMD) and the surrounding free-living (FL)
40 and organic particle-attached (PA) lifestyles sampled during the *Tara* expeditions in two of the
41 most plastic polluted zones in the world Ocean, i.e. the North Pacific gyre and the
42 Mediterranean Sea. The 16S rRNA gene sequencing analysis confirmed that PMD are a new
43 anthropogenic ocean habitat for marine microbes at the ocean-basin-scale, with clear niche
44 partitioning compared to FL and PA lifestyles. At an Ocean-basin-scale, the composition of the
45 plastisphere communities was mainly driven by environmental selection, rather than polymer
46 types or dispersal effect. A plastisphere 'core microbiome' could be identified, mainly
47 dominated by *Rhodobacteraceae* and *Cyanobacteria*. Predicted functions indicated the
48 dominance of carbon, nitrogen and sulfur metabolisms on PMD that open new questions on the
49 role of the plastisphere in a large number of important ecological processes in the marine
50 ecosystem.

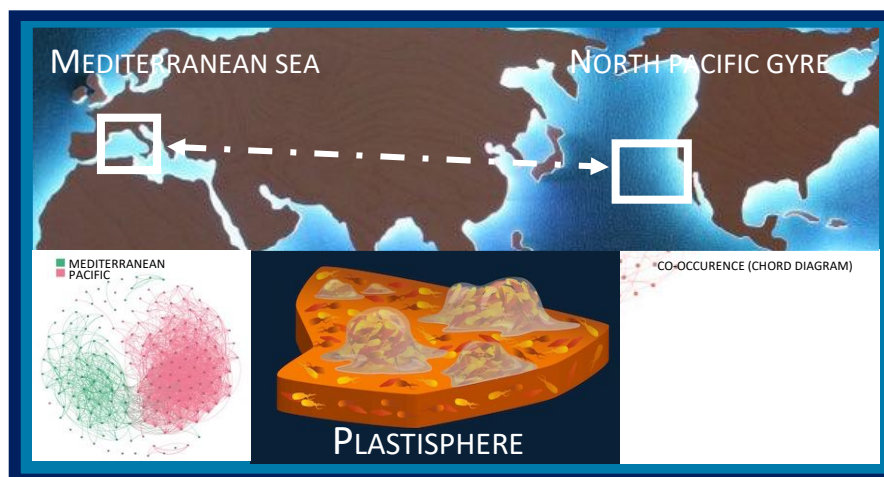
51

52 **Highlights:**

- 53 • Niche partitioning on plastic marine debris (PMD) at the ocean-basin-scale
- 54 • Environmental selection rather than plastic dispersion drives plastisphere bacterial diversity
- 55 • A plastisphere 'core microbiome' dominated by *Rhodobacteraceae* and *Cyanobacteria*
- 56 • Dominance of carbon, nitrogen and sulfur metabolisms on PMD

57

58 **Graphical abstract**



59

60 **1. Introduction**

61 Plastics are part of the emerging pollutants and they are now regarded as a key geological
62 indicator of the Anthropocene because of their abundance and widespread distribution on Earth
63 (Zalasiewicz et al. 2016). The ocean represents the final destination of mismanaged terrestrial
64 plastic waste, with an estimated 500,000 tons of plastic entering the sea each year (Kaandorp et
65 al. 2023). Plastic stocks at the world's upper oceans amount from 82 to 578 of kilotons (Isobe
66 et al. 2021), mainly dominated by <5mm in size microplastics coming from the fragmentation
67 of larger items (ter Halle et al. 2016). Vast accumulation zones of buoyant plastic were
68 described in the five main oceanic gyres, including the most famous 'Great Pacific garbage
69 patch' in the North Pacific Ocean where up to the order of kilograms (or millions of pieces) per
70 km² was found in the center of the gyre (Lebreton et al. 2018). The Mediterranean Sea has been
71 proposed as the sixth great accumulation zone for marine litter, with some of the highest
72 concentrations of floating plastics in the world (Cozar et al. 2014).

73 Plastics represent physical support for microbial life, the so-called 'plastisphere' (Zettler
74 et al. 2013). A range of 1 to 15 kilotons of microbial biomass has been estimated harbored on
75 the plastic marine debris (PMD), which is in the same range as the estimated microbial carbon
76 mass in the global rivers or both polar regions (Zhao et al. 2021). The plastisphere has several
77 independent or cumulative effects on the fate and impacts of plastic in the marine environment.
78 The biofouling may increase the sedimentation of the plastic particles by decreasing its
79 buoyancy (Kooi et al. 2017; Kane et al. 2020). It is disguising the plastic pieces, thus creating
80 particles more similar to food items for grazers (Vroom et al. 2017). Biofilm growing on plastics
81 has been recently shown to alter the biogeochemical cycles of elements by consuming and
82 releasing nutrients (Chen et al. 2020) and favor the colonization by algae (Nava and Leoni
83 2021) or metazoan larvae (Ghiglione and Laudet 2020), thus helping indirectly the spread of
84 non-indigenous species over large geographic distances by plastic dispersion (Miralles et al.
85 2018). The detection of potentially pathogenic *Vibrio* species (such as *V. aestuarianus* and *V.*
86 *splendidus*) classically found in the plastisphere also raised the question of the diffusion of
87 infectious diseases by plastics (Pedrotti et al. 2022). Finally, the plastic biofilms were shown to
88 host hydrocarbonoclastic bacteria that are thought to be involved in their biodegradation
89 processes (Jacquin et al. 2019).

90 Bacteria living on plastics have demonstrated distinct niche partitioning in comparison to
91 their counterparts living in organic-particle attached and free-living lifestyles (Dussud et al.
92 2018a), as well as compared to microorganisms residing on other substrates like wood,
93 cellulose, or glass (Kirstein et al. 2018; Oberbeckmann et al. 2018; Ogonowski et al. 2018).

94 The reasons for this preferential attachment on plastic particles are still enigmatic. The early
95 stages of colonization may be influenced significantly by factors such as hydrophobicity,
96 topography, roughness, crystallinity, and surface charge (Rummel et al. 2017). However,
97 bacterial communities composing a mature biofilm can undergo alterations, as demonstrated by
98 the occurrence of a diatom bloom on plastic surfaces due to environmental changes (Cheng et
99 al. 2020). The majority of research conducted on the plastisphere was based on controlled
100 incubation experiments using plastics with known compositions, and only a few investigated
101 plastic debris collected at sea, and even fewer were conducted specifically in the open ocean
102 (Amaral-Zettler et al. 2020). This lack of knowledge explains that no consensus has been
103 reached so far to explain the preferential attachment of some bacteria on plastics. Although
104 numerous recent studies have made efforts to characterize the plastisphere niche partitioning, it
105 is still not clear whether a core microbiome (microbial taxa shared by all plastic substrates) can
106 contribute to the description of the plastisphere in the marine environment. Few studies have
107 explored the core plastisphere microbiome in naturally occurring plastic litters from distinct
108 marine geographical areas (Aguilla-Torres et al. 2022, Basili et al. 2020), but these have been
109 carried out on a regional scale and never in distinct geographically distant oceanic regions.

110 Here, we explored the biogeography of the plastisphere from samples collected during
111 two *Tara* expeditions the most plastic polluted oceanic regions on Earth, i.e., the North Pacific
112 gyre and the Mediterranean Sea. We hypothesized that the preferential attachment of some
113 bacterial species on plastics, as compared to the surrounding free-living and organic particle-
114 attached communities, may be conserved within and between the two distinct environmentally
115 and geographically distant oceanic regions. We also hypothesized that a plastisphere core
116 microbiome may be identified across both regions, which may help to identify and understand
117 critical factors and functions driving the specificity of microbial communities living on plastic
118 debris.

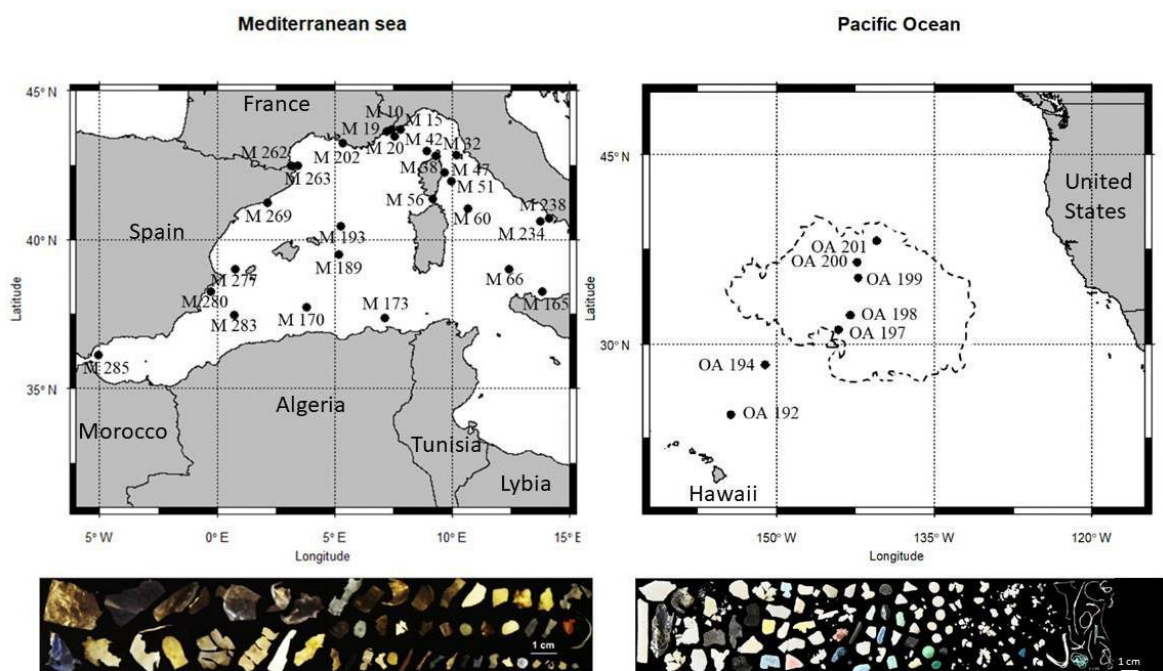
119

120 **2. Materials and Methods**

121 **2.1. Sampling plastic marine debris and the surrounding sea water**

122 Samples were taken using the same protocol during two cruises aboard the research vessel
123 *Tara* in the Western Mediterranean Sea (*Tara* Mediterranean expedition from April to
124 November 2014) and in the North Pacific gyre (*Tara* Pacific expedition from June to July 2018)
125 (**Fig. 1**). Plastic marine debris (PMD) floating in surface waters were gathered by utilizing a
126 manta net with a 330 μm mesh attached to a frame and trawled behind the boat for 30 minutes
127 to an hour at a speed of 3 knots. At each of the 39 sampling stations, a subset of the plastic items

128 of various sizes (ranging from a few mm² to a few cm²), colors and textures (**Fig. 1**) were sorted
 129 under a dissecting microscope using sterilized forceps and immediately frozen in liquid nitrogen
 130 until further analysis. Prior to deploying each manta net, a conductivity-temperature-
 131 fluorescence-depth profiler (CTD – SeaBird SBE 19, in the first 100 m below the surface) and
 132 a Niskin bottle for collecting surface seawater (in the first meter below the surface) were
 133 deployed at each station. A total of 2 L of seawater was sequentially filtered through 3 µm-pore
 134 size polycarbonate filters (referred to as the particle-attached fraction, PA) and 0.2 µm-pore
 135 size polycarbonate filters (referred to as the free-living fraction, FL) using a peristaltic pump
 136 (pressure <100 mbar). Filters were immediately frozen in liquid nitrogen until DNA extraction.



137
 138 **Figure 1:** Station locations in the Western Mediterranean Sea (left part, n=32) and in the North Pacific
 139 Ocean (right part, n=7). The corresponding light-micrograph of the 218 PMD collected at each oceanic
 140 region is presented below each map, respectively (114 particles collected in the western Mediterranean
 141 Sea and 104 in the North Pacific gyre). The mapping of the North Pacific gyre (dotted line) is indicated
 142 according to Lebreton et al. (2018).

143

144 2.2. DNA extraction, PCR and sequencing

145 A first set of 218 DNA extractions was done using the individual PMD sampled in the
 146 North Pacific gyre (n=104, between 3 and 38 plastic pieces analyzed per station) and in the NW
 147 Mediterranean Sea (n=114, between 2 and 4 plastic pieces analyzed per station). A second set
 148 of 39 DNA extracts were obtained from all 3 µm- (particle-attached, PA) and 0.2 µm-pore size

149 filters (free-living, FL) from the surrounding seawater (n=7 stations in the North Pacific gyre
150 and n=32 stations in the Western Mediterranean Sea). The DNA extraction process utilized a
151 standard phenol-chloroform-based protocol (Anderson et al. 1983) with the addition of
152 preliminary steps for plastics, as previously described (Dussud et al. 2018b). Briefly, cell
153 detachment using a sonication pre-treatment (3 x 5 s with 30% amplitude, Branson SLPe) was
154 performed for the disruption of the biofilm in order to improve the further enzymatic and
155 chemical cell lysis of the biofilm (1 mg mL⁻¹ lysozyme at 37°C for 45 min followed by 0.2 mg
156 mL⁻¹ proteinase K and 1% SDS at 50°C for 1 h).

157 Sequencing was performed using Illumina MiSeq at the Genoscope (Paris, France) after
158 PCR amplification of the 16S rRNA V4–V5 region using 515-FY and 926-R primers (Parada
159 et al. 2016). Raw FASTA files were deposited at NCBI (accession numbers PRJEB58218 and
160 PRJEB52329). The 16S rRNA gene sequences were analyzed using the FROGS pipeline host
161 in the Galaxy platform (Escudié et al. 2018), as previously described (Odobel et al. 2021).
162 Briefly, the merge the paired-ends raw reads were clustered using the SWARM algorithm
163 (Mahé et al. 2014) after quality filtering and primers trimming with cutadapt (Martin, 2011).
164 The removal of chimera was performed after detection by de novo UCHIME method with the
165 VSEARCH algorithm (Edgar et al., 2011; Rognes et al., 2016). Operational Taxonomic Units
166 (OTUs) were defined after clustering (0.03 distance threshold) and further assignment with the
167 Silva128 16S rRNA database (Quast et al., 2012). Chloroplast and mitochondrial sequences as
168 well as clusters that did not belong to Bacteria kingdom were removed.

169

170 **2.3. Characterization of each PMD**

171 After the cell lysis step of DNA extraction, each individual PMD was processed using the
172 ImageJ software in order to determine the one-dimensional surface area, major length, and
173 circularity. Additionally, the chemical analysis of each PMD was conducted using the
174 Attenuated Total Reflection Fourier Transform Infrared spectrometer (ATR-FTIR Spectrum
175 100, Perkin-Elmer) and the polymer composition was determined using the POSEIDON
176 software (Kedzierski et al. 2019).

177

178 **2.4. Statistical analysis and diversity assessment**

179 The confidence interval (*IC*) for the proportion of polymer composition in the sampled
180 plastics at each station and the *IC* for the carbonyl index (CI) and hydroxyl index (HI) of the
181 PE-based PMD were calculated following the method described by Kedzierski et al. (2019).

182 It is to be expected that the count of unique sequences (and hence OTUs) detected in a

183 sample will rise with the total number of sequences reads, which may fluctuate according to the
184 sequencing efficiency for each sample (Gilbert et al. 2009). To ensure accurate data
185 comparisons, the bacterial 16S rRNA sequences in each sample were randomly subsampled to
186 match the number of sequences in the sample with the fewest sequences (N=9,115). We decided
187 to remove four samples from the global dataset (with less than 9,115 sequences per sample, and
188 thus not taken into account for further processing), and all the remaining samples stayed in the
189 stationary phase of the rarefaction curve after resampling. All the subsequent results were
190 calculated using this standardized dataset with 9,115 sequences per sample (Ghiglione and
191 Murray 2012). The non-parametric Chao1 species richness estimator (SPADE software;
192 Bandinelli et al. 1993), along with the Shannon diversity and Pielou evenness indices
193 (PRIMER-E; Clarke and Warwick 2001), were used to estimate alpha-diversity. Differences
194 between FL, PA and PMD bacterial richness, evenness and diversity indices were tested using
195 non-parametric Kruskal-Wallis test (package 'stats' version 3.3.1, RStudio software version
196 1.0.143). For beta-diversity analysis, a non-metric multidimensional scaling (NMDS) on two
197 dimensions was generated based on Bray-Curtis dissimilarity. Statistical analysis of similarities
198 between groups (ANOSIM, PRIMER-E) was used for a combination of natural and Plastic
199 related "niche" lifestyles (FL/PA or PMD) with ocean provenance (Mediterranean Sea vs.
200 Pacific Ocean). ANOSIM is a nonparametric technique designed to allow statistical
201 comparisons for multivariate data sets in a manner similar to univariate techniques (ANOVA)
202 (Clarke and Warwick, 2001). Both NMDS and ANOSIM were performed using the vegan R
203 package (Oksanen et al. 2015).

204 We utilized the direct gradient approach canonical correspondence analysis (CCA,
205 CANOCO 4.5) to examine the relationships between bacterial community structure and various
206 environmental parameters (pressure, temperature, conductivity, salinity, oxygen and
207 photosynthetically available radiation from CTD - SeaBird SBE 911 data), geographical
208 distance between samples and PMD characteristics (polymer composition and oxidation level
209 from FTIR data, as well as surface and major length of the individual PMD from ImageJ
210 software), as previously described (Ghiglione et al. 2008). The significance of the
211 environmental variables was determined through Spearman rank pairwise correlations.

212

213 **2.5. Core microbiomes identification, co-occurrence networks inference and predicted** 214 **metagenomes**

215 Venn diagrams were obtained by identifying the set of OTUs present in each of the
216 Mediterranean and the Pacific fractions using R software (R 5.6.3) and a representation of the

217 histogram was made using Excel software. The core microbiome was identified by the common
218 OTUs in the two fractions characterized by the overlapping circles.

219 A co-occurrence network for PMD samples was inferred using the FlashWeave package
220 (Tackmann et al. 2019). To check effects due to the imbalance between Mediterranean and
221 Pacific samples, we randomly selected 75 out of 104 Pacific samples and built co-occurrence
222 networks using the same parameters. Furthermore, the network was decomposed into modules
223 using the leading eigenvectors algorithm (Clauset et al. 2004). Briefly, this algorithm finds
224 communities that maximize modularity, a network property that accounts for the number of
225 edges falling within groups minus the expected number in an equivalent network with edges
226 placed at random (Newman 2006). As a result, modules detected by the leading eigenvector
227 algorithm maximize the number of edges within modules and minimize the connections
228 between modules.

229 Metagenome prediction was performed using the PICRUS2 software (Douglas et al.
230 2020). To detect enriched pathways, we compared the relative abundance of each pathway in
231 each sample. Next, after CLR transformation, we used a Kruskal-Wallis test to detect
232 differences in means (FDR adjustment, q -value $< 1e-3$), followed by a Dunn post-hoc test to
233 attribute which pathway is enriched in which sample group (ocean-niche).

234

235 **3. Results**

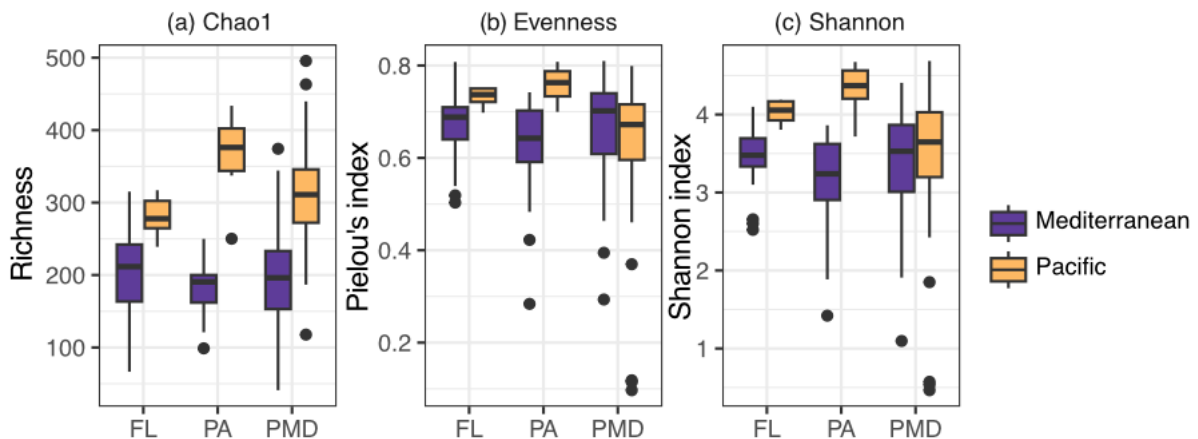
236 **3.1. Chemical characterization showed dominance of PE-based plastics in both oceanic** 237 **regions**

238 ATR-FTIR analyses showed that polyethylene (PE) dominated the composition of the
239 sorted PMD in both the Western Mediterranean Sea and in the North Pacific Gyre, with
240 $66.1 \pm 10.3\%$ and $71.1 \pm 8.7\%$, respectively. In the Mediterranean Sea, PE was followed by
241 propylene (PP; $21.2 \pm 6.2\%$) and polystyrene (PS; $4.2 \pm 3.1\%$), with other polymers representing
242 $3.6 \pm 2.8\%$ and undetermined were $4.9 \pm 3.3\%$. Similar proportions were found in the North
243 Pacific Gyre with PP ($16.0 \pm 7.0\%$) followed by PS ($5.3 \pm 4.3\%$) and other polymers ($5.3 \pm 5.1\%$),
244 with undetermined at $2.3 \pm 2.9\%$. The PP/PE ratio is higher in the Mediterranean Sea (0.32) than
245 in the North Pacific Gyre (0.23). Based on PE spectra, no significant differences were found
246 between the carbonyl index (CI) in the Mediterranean Sea and Pacific gyre (CI = 0.78 ± 0.16 and
247 0.78 ± 0.11 , respectively), whereas significant differences were found for the hydroxyl index HI
248 (Mediterranean Sea: 5.7 ± 1.1 ; Pacific gyre: 2.5 ± 0.5) and the fouling index FI (Mediterranean
249 Sea: 1.0 ± 0.24 ; Pacific gyre: 0.29 ± 0.04).

250

251 **3.2. Comparison of α -diversity indexes between the FL, PA and PMD lifestyles in the**
252 **Mediterranean and Pacific regions**

253 The Chao1 index indicated that the bacterial richness was significantly higher in the North
254 Pacific gyre compared to the Mediterranean Sea for all FL, PA and PMD lifestyles (Man-
255 Withney $p < 2.2 \cdot 10^{-16}$) (**Fig. 2**). Significant differences were found between the three groups
256 within each oceanic region (Mann Withney $p < 0.05$), but with different trends depending on the
257 geographic region. The PMD (170.1 and 262.3) presented always intermediate Chao1 estimated
258 richness values compared to FL (174.4 and 251.0) and PA (153.8 and 323.0).



259
260 **Figure 2:** Comparison of α -diversity indices: (a) Chao1 richness, (b) Pielou evenness and (c) Shannon
261 diversity indexes between the FL, PA and PMD lifestyles according to the sampling location (Western
262 Mediterranean Sea and North Pacific gyre). The median values are marked with a vertical line, and
263 whiskers represent the minimum and maximum values. Outliers are indicated as filled circles.

264
265 The Pielou evenness index was similar for the PMD in the Mediterranean and the Pacific
266 regions (Man-Whitney, $p=0.4$), whereas significant differences were found for PA and FL
267 lifestyles between the two oceanic regions ($p=4.1 \cdot 10^{-4}$ and $p=2.5 \cdot 10^{-2}$, respectively). No
268 significant differences were observed between PMD, PA and FL in the Mediterranean Sea
269 (Kruskal and Wallis, $p=0.24$; mean values of 0.67, 0.62 and 0.68, respectively), whereas
270 significant differences were found in the Pacific (Kruskal and Wallis, $p=7.2 \cdot 10^{-5}$; mean values
271 of 0.64, 0.76 and 0.73 on PMD, PA and FL, respectively).

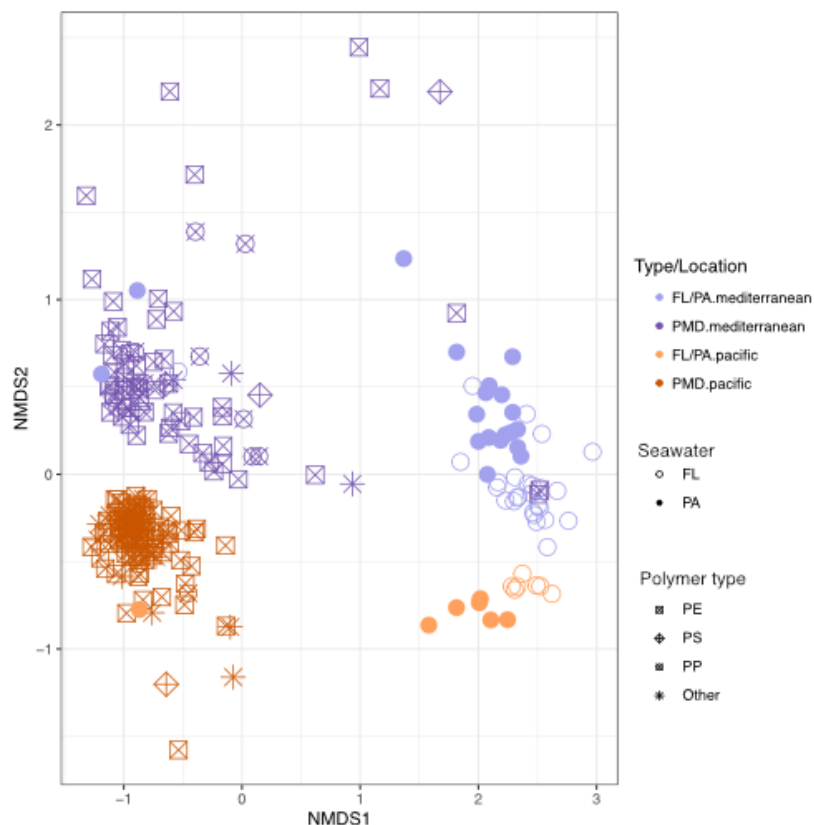
272 The Shannon index confirmed a significantly higher microbial diversity in the North
273 Pacific gyre compared to the Western Mediterranean samples (Kruskal and Wallis, $p=7.6 \cdot 10^{-5}$)
274 for the FL (Shannon index average values of 4.03 and 3.42, respectively) and PA (4.33 and

275 3.14, respectively), but not for the PMD (Shannon index average values of 3.52 and 3.41,
276 respectively; Mann-Withney $p=0.13$).

277

278 3.3. Bacterial community structure (β -diversity) with high dissimilarities between PMD 279 compared to FL and PA lifestyles

280 Clustering according to the three sample lifestyles clearly emerged with higher
281 differences between PMD compared to FL and PA lifestyles (**Fig. 3**). Each group could be
282 divided into two subgroups according to their geographical origin, i.e., Mediterranean Sea or
283 North Pacific gyre (NMDS2 axis). Remarkably, PMD communities were not structured by
284 plastic type (**Fig. 3**). In order to confirm the visual cluster separation from Figure 3, we run a
285 nonparametric ANOSIM test. The analysis showed a significant separation between groups
286 (ANOSIM $R=0.67$, $p=0.001$) when using lifestyle/ocean grouping (i.e., FL/PA.Mediterranean,
287 PMD.Mediterranean, FL/PA.Pacific, PMD.Pacific). Furthermore, a detailed ANOSIM pairwise
288 comparison between groups (**Suppl. Table 1**) indicated less difference in FL/PA vs. PMD in
289 the Mediterranean Sea vs. the Pacific Ocean samples.



290

291 **Figure 3.** Non-metric multidimensional scaling (NMDS) plot based on Bray-Curtis similarities of
292 bacterial communities (stress = 0.10) of PMD (hollow shapes in non-muted colors, together with
293 information of the polymer type, i.e. PE, PP, PS and others), FL and PA (solid squares or triangles with

294 muted colors, respectively). Ocean provenance is depicted in violet or orange for the Western
295 Mediterranean Sea and the North Pacific Ocean, respectively.

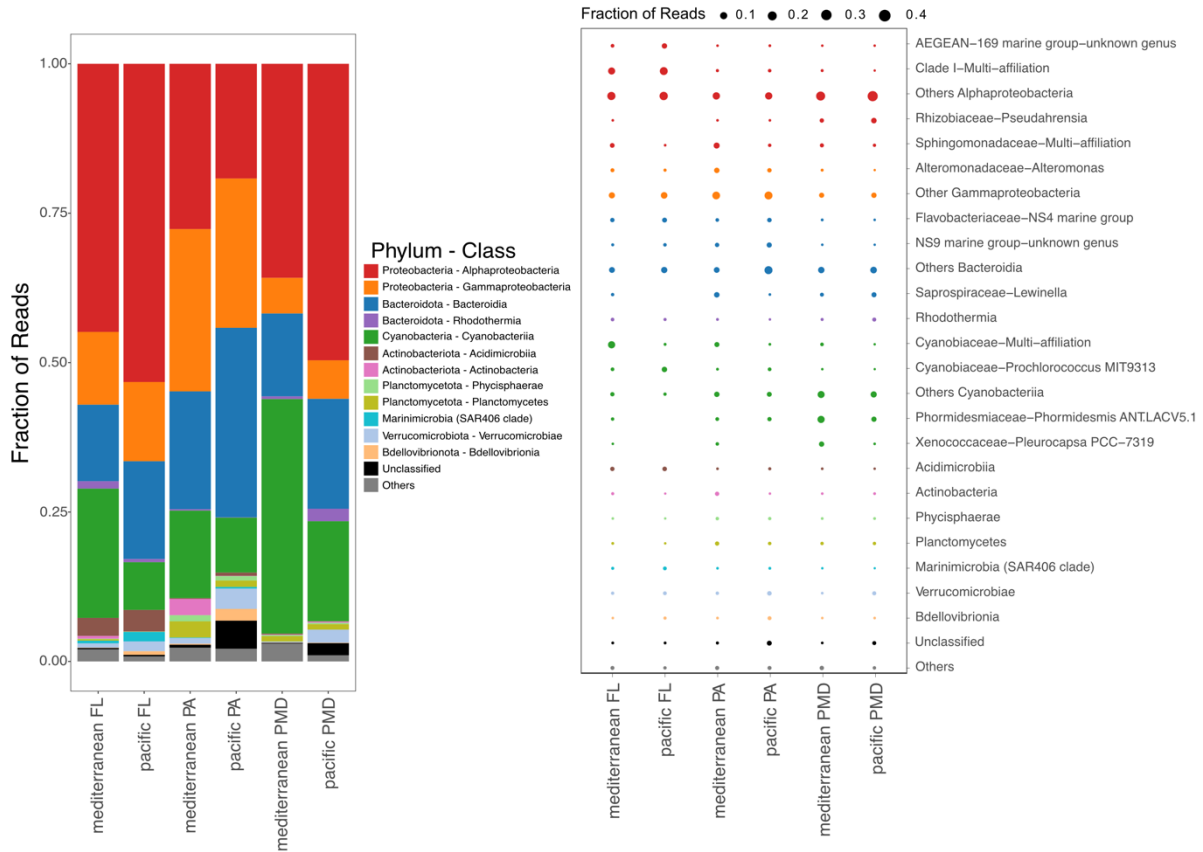
296

297 **3.4. Taxonomic affiliation and similarity analysis of FL, PA and PMD lifestyles between** 298 **the Mediterranean and Pacific regions**

299 The FL lifestyle was dominated by *Alphaproteobacteria* that represented 45% in the
300 Mediterranean Sea and 53.24% in the North Pacific gyre, with *SAR11* as the dominant group
301 (14.63% and 25.5% of the total relative abundance in the two oceanic regions, respectively)
302 together with *Rhodobacteraceae* (6.0% in Pacific and 6.84% in Mediterranean) (**Fig. 4**).
303 Cyanobacteria represented a higher proportion of the community in the FL Mediterranean Sea
304 (21.6%) than in the North Pacific gyre (8.0%), with *Prochlorococcus* sp. as the dominant group
305 (1.43% and 6.86% of the total relative abundance in the two oceanic regions, respectively).
306 *Bacteroidia* were also very abundant in the FL (16.9% in the Pacific and 26.5% in the
307 Mediterranean) with the dominance of *Flavobacteriaceae* (11.6% in the Pacific and 9.36% in
308 the Mediterranean). Inversely, *Bacteroidia* (mainly *Flavobacteriaceae*) and
309 *Gammaproteobacteria* were more abundant in the North Pacific gyre (16.0% and 13.2%,
310 respectively) than in the Mediterranean Sea (12.8% and 12.2%, respectively). Similarity
311 percentage analysis (SIMPER) showed that *Cyanobiaceae* explained 14.44% of the difference
312 between the two oceanic regions (higher abundance in the Mediterranean Sea), whereas
313 *Prochlorococcus* sp. and *Rhosospirillales* explained 5.2 and 4.4%, respectively (higher
314 abundance in the Pacific).

315 The PA lifestyle was also dominated by the same four taxonomic groups
316 (*Alphaproteobacteria*, *Gammaproteobacteria*, *Cyanobacteria* and *Bacteroidia*), but with
317 different proportions between locations and compared to FL (**Fig. 4**). The proportion of
318 *Bacteroidia* increased in the PA compared to FL, and became even dominant in the North
319 Pacific gyre with 31.7% of the total affiliated reads (mainly *Formosa* sp. and *Fluviicola* sp.),
320 while it represented only 20% in the Mediterranean Sea (mainly *Lewinella* sp.). The proportion
321 of *Alphaproteobacteria* was lower in the North Pacific gyre (19.2%, mainly composed of
322 *Rhodobacteraceae* family) as compared to the Western Mediterranean Sea (27.6%, mainly
323 composed of *Sphingomonadaceae* family), whereas it was similar in both oceanic regions for
324 *Gammaproteobacteria* (25% and 27%, respectively, mainly *Alteromonas* sp.). *Cyanobacteria*
325 represented 9.18% in the North Pacific gyre (mainly *Phormidesmiaceae*) and 14.62% in the
326 Western Mediterranean Sea (mainly *Cyanobiaceae*). The SIMPER analysis showed that
327 *Sphingomonadaceae*, *Alteromonadaceae* and *Lewinella* sp. explained 5.5%, 5.24% and 4.36%

328 of the dissimilarity in PA between the two oceanic regions of both regions, respectively (higher
 329 abundance in the Mediterranean Sea). The North Pacific PA lifestyle is distinguished from the
 330 Mediterranean PA lifestyle by a high abundance of the genus *Formosa* sp. (1.4%), *Alteromonas*
 331 sp. (1.1%) and *Fluviicola* sp. (1.29%) (not shown on the bubble plot, percentage dissimilarity
 332 < 5%).



333
 334 **Figure 4.** Bacterial OTUs associated with the FL, PA and PMA lifestyles in the Mediterranean Sea and
 335 in the North Pacific gyre. Left panel: relative abundance of the major groups at the Phylum-Class level.
 336 Right panel: Main Family-Genus levels explaining differences (assessed by SIMPER). Others: 1.88% of
 337 total reads, Unclassified: 1.11% of total reads.

338
 339 The PMD lifestyle contained a drastically lower proportion of *Gammaproteobacteria*
 340 compared to PA and FL, which represented only 5.94% and 6.43% of the average abundance
 341 across PMD samples in the Mediterranean Sea and in the North Pacific gyre, respectively (**Fig.**
 342 **4**). *Cyanobacteria* were much more abundant on PMD in the Mediterranean Sea (39.2%) as
 343 compared to the North Pacific gyre (15.0%), where others were present in both regions, such
 344 as *Phormidemis* sp. (16.4% and 6.1%, respectively), *Rivularia* sp. (9.3% and 9.0%,
 345 respectively) and *Pleurocapsa* sp. (6.2% and 0.08%, respectively). Inversely,
 346 *Alphaproteobacteria* were much less abundant in the Mediterranean Sea (35.8%) compared to

347 the North Pacific gyre (54.5%), where several members of the *Rhodobacteraceae* were
348 abundant in both oceanic regions (19.8 and 30.5%, respectively), including *Pseudahrensia* sp.
349 (2.9% and 7.3%, respectively), *Tateyamaria* sp. (2.4% and 4.1%, respectively) and
350 *Erythrobacter* sp. (3.3% and 1.4%, respectively). Finally, *Bacteroidetes* were found in similar
351 proportion in the Mediterranean Sea (13.9%) as compared to the North Pacific gyre (15.0%),
352 dominated by *Flavobacteriaceae* (9.8% and 8.7%, respectively), *Saprospiraceae* (2.84% and
353 7.5%, respectively) and *Rhodothermaceae* (0.4% and 1.84%, respectively), including
354 *Muricauda* sp. (1.2% and 1.7%, respectively) and *Lewinella* sp. (1.9% and 5.4%, respectively).
355 SIMPER analysis confirmed that the OTUs explaining 35 % of the difference between the PMD
356 communities living in both oceanic regions were *Phormidesmis* sp., *Pleurocapsa* sp.,
357 *Erythrobacter* sp., *Acrophormium* sp., *Dokdonia* sp. and *Sagittula* sp. that were more abundant
358 in the Mediterranean Sea (explaining 20.3% of the variability) and *Pseudahrensia* sp.,
359 *Lewinella* sp., *Psychrobacter* sp., *Tenacibaculum* sp., *Roseovarius* sp. and *Cobetia* sp. in the
360 North Pacific gyre (explaining 14.7% of the variability). The SIMPER analysis also revealed
361 that *Cyanobiaceae*, *Phormidesmis* sp., *SAR11* and *Rivularia* sp. explained together 31.5% of
362 the dissimilarity between PMD and FL in the Mediterranean Sea, and *SAR11*, *Rivularia* sp. and
363 *Pseudahrensia* sp. explained 20.5% in the North Pacific gyre. Distinction between PMD and
364 PA were explained at 30.0% by *Phormidesmis* sp., *Rivularia* sp. Alteromonadaceae,
365 Sphigomonadaceae and *Lewinella* sp. in the Mediterranean Sea, whereas *Rivularia* sp.,
366 *Phormidesmis* sp. and *Pseudahrensia* sp. explained 13.1% of the dissimilarity in the North
367 Pacific gyre.

368

369 **3.5. Temperature and geographical distance are the main factors driving FL, PA and** 370 **PMD bacterial community structure in both oceanic regions**

371 Canonical correspondence analysis (CCA) revealed that a combination of multiple
372 regression on matrix analysis using environmental factors and geographical distance accounted
373 for 26.7% (FL lifestyle), 17.6% (PA lifestyle), and 16.8% (PMD lifestyle) of the overall
374 variation in the Bray-Curtis dissimilarity matrix (**Table 1**). The effect of environmental
375 variables on bacterial community structure was statistically significant ($p < 0.05$) for the FL
376 (14.3% of the variance), PA (7.6% of the variance) and PMD lifestyles (6.5% of the variance).
377 Temperature was the main environmental driver in all the lifestyles (9.9%, 4.8% and 4.4% of
378 the variance in FL, PA and PMD, respectively). Geographical distance between samples was
379 also significant and explained a high proportion of the variance for all lifestyles (12.4%, 10.0%
380 and 10.3% of the variance in FL, PA and PMD, respectively; $p < 0.05$).

	FL	PA	PMD
Physico-chemical (seawater)	14.3	7.6	6.5
Temperature only	9.9	4.8	4.4
Geographical distance	12.4	10.0	10.3
Total variance Env	26.7	17.6	16.8
PMD characteristics	ND	ND	3.6

381

382 **Table 1.** Percentage of variance explained by CCA analysis of the bacterial community structure data
383 when constrained by physico-chemical variables (temperature, salinity, oxygen and PAR), geographical
384 distance and/or PMD characteristics (polymer composition, oxidation level, surface and major length).
385 All values were significant ($p < 0.05$) when using a Monte Carlo permutation full model test (199
386 permutations). ND: non-determined.

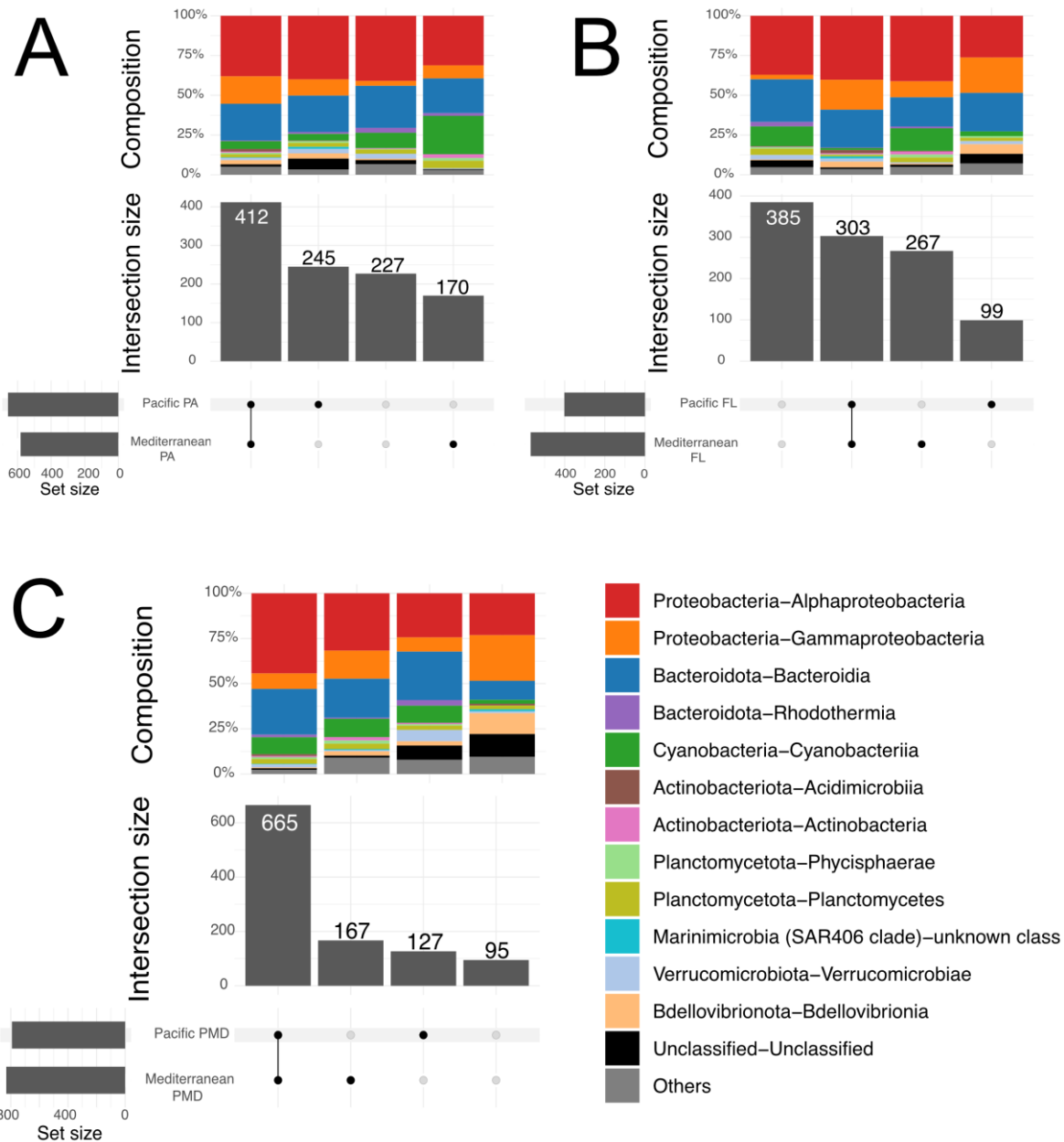
387

388 3.6. Identifying core microbiomes on FL, PA and PMD across oceanic regions

389 With the objective to identify and describe core microbiomes in FL, PA and PMD
390 lifestyles, we first analyzed OTUs shared among bacterial consortia living in both the oceanic
391 regions, represented by UpSet plots (**Fig. 5**). A core microbiome was identified for the FL
392 samples, representing 303 OTUs (45% of all OTUs) composed of *Alphaproteobacteria* (51%),
393 mainly represented by the order *SAR11* (27.45%), *SAR116* (6.5%), *Rhodobacteraceae* (6.26%)
394 and *Sphingomonadaceae* (2.5%). *Gammaproteobacteria* represented nearly 17.7% of the FL
395 core microbiome, mainly represented by the order *SAR86* (4.22%) and the *Alteromonadaceae*
396 family (2.86%), of which the genus *Alteromonas* sp. is very dominant (1.5%). The
397 *Cyanobacteria* represented 14.5%, with *Cyanobiaceae* and the genus *Prochlorococcus* sp.
398 (4.5%). *Bacteroidia* were found at 13.1% of the entire core microbiome, mainly represented by
399 the *Flavobacteriaceae* (10%) including the *Formosa* sp. (0.85%) and *Fluviicola* sp. (0.34%).

400 The core microbiome of 412 OTUs in PA samples (49% of all OTUs) was dominated by
401 *Gammaproteobacteria* (30.5%), mainly *Alteromonadaceae* (18.02%) including *Alteromonas*
402 sp. (4.5%) and *Aesturiibacter* sp. (2.26%). *Alphaproteobacteria* represented 24.5% of the PA
403 core microbiome, represented by the *Rhodobacteraceae* (8.7%, including *Parococcus* sp. and
404 *Ruegeria* sp.), *Sphingomonadaceae* (7.7%, mainly *Sphingobium* sp.), and *Rhizobiaceae* (1.4%,
405 mainly *Fulvimarina* sp.). *Bacteroidia* represent 28.05% of the PA core microbiome, mainly
406 composed of *Saprospiraceae* (4.9%, mainly *Lewinella* sp.), *Flavobacteriaceae* (12.7%,
407 including *Formosa* sp. and *Fluvicola* sp.). Finally, *Cyanobacteria* represents only 8.8% of the
408 PA core microbiome, mainly represented by the *Cyanobiaceae* (4.8%, mainly *Prochlorococcus*
409 sp. and *Phormidesmiaceae*).

410 In the PMD lifestyle, 665 OTUs was shared between both oceanic regions, a higher
411 percentage (69%) compared to FL and PA lifestyles. This core microbiome within the PMD
412 samples was dominated by *Alphaproteobacteria* (45.35%), followed by *Cyanobacteria*
413 (28.8%), *Bacteroidia* (14.9%) and *Gammaproteobacteria* (6.25%). *Alphaproteobacteria* was
414 mainly represented by *Rhodobacteraceae* (27%, mainly *Tateyamaria* sp., *Yoonia-Loktanella*
415 sp. and *Sagitula* sp.), *Rhizobiaceae* (9.34%, mainly *Pseudahrensia* sp.) and
416 *Sphingomonadaceae* (4.44%, mainly *Erythrobacter* sp. and *Sphingobium* sp.). *Cyanobacteria*
417 were dominated by Phormidesmiaceae (13.13%, mainly *Phormidesmisis* sp.), Rivulariaceae
418 (10.55%, mainly *Calothrix parasitica* and *Calothrix* sp.) and *Xenococcaceae* (3.06%, mainly
419 *Pleurocapsa* sp.). *Bacteroidia* were dominated by *Flavobacteriaceae* (8.7%, mainly *Muricauda*
420 sp., *Dohdonia* sp. and *Winogradskyella* sp.) and *Saprospiraceae* (5%, mainly *Lewinella* sp.).
421 *Gammaproteobacteria* were dominated by the *Moraxellaceae* (2.28%, mainly *Acinetobacter*
422 sp. and *Psychrobacter* sp.) and *Halomonadaceae* (0.92%, mainly *Cobetia* sp. and *Halomonas*
423 sp.). Other families were also present such as the *Nostocaceae* (belonging to *Cyanobacteria*
424 30.2%), as well as the *Rhizobiaceae* (13%), *Sphingomonadaceae* (8.3% of the core
425 microbiome) and *Hyphomonadaceae* (3.5%). The most represented genus in the PMD core
426 microbiome was *Rivularia* sp. (belonging to the *Nostocaceae* family), followed by
427 *Pseudahrensia* sp. (13%; belonging to the *Pseudahrensia* sp. family. In the *Rhodobacteraceae*
428 family, the genus *Tateyamaria* sp. and *Roseovarius* sp. represented 14% of the PMD core
429 microbiome. The *Sphingomonadaceae* family was represented by the *Erythrobacter* sp., which
430 represents 5.4% of the PMD core microbiome. Interestingly, we could not identify any
431 persistent OTUs that was consistently detected in 100% of the PMD samples. When arbitrarily
432 decreasing the cut-off to 90%, we found only 17 OTUs belonging mainly to the
433 *Rhodobacteraceae* family, representing 45% of the abundance of the core microbiome families.



434

435 **Figure 5:** UpSet Plots from PA (A), FL (B) and PMD lifestyles found in the Mediterranean Sea and
 436 North Pacific gyre. Black dots represents the set of OTUs in either North Pacific gyre (upper black dot),
 437 the Mediterranean Sea (low black dot), their intersection (connected black dots) or not in the
 438 corresponding lifestyle (disconnected grey points). Grey bars show the number of OTUs per set and
 439 colored bars their composition in Phylum – Class categories.

440

441 3.7. A global PMD co-occurrence network for the Mediterranean and Pacific regions

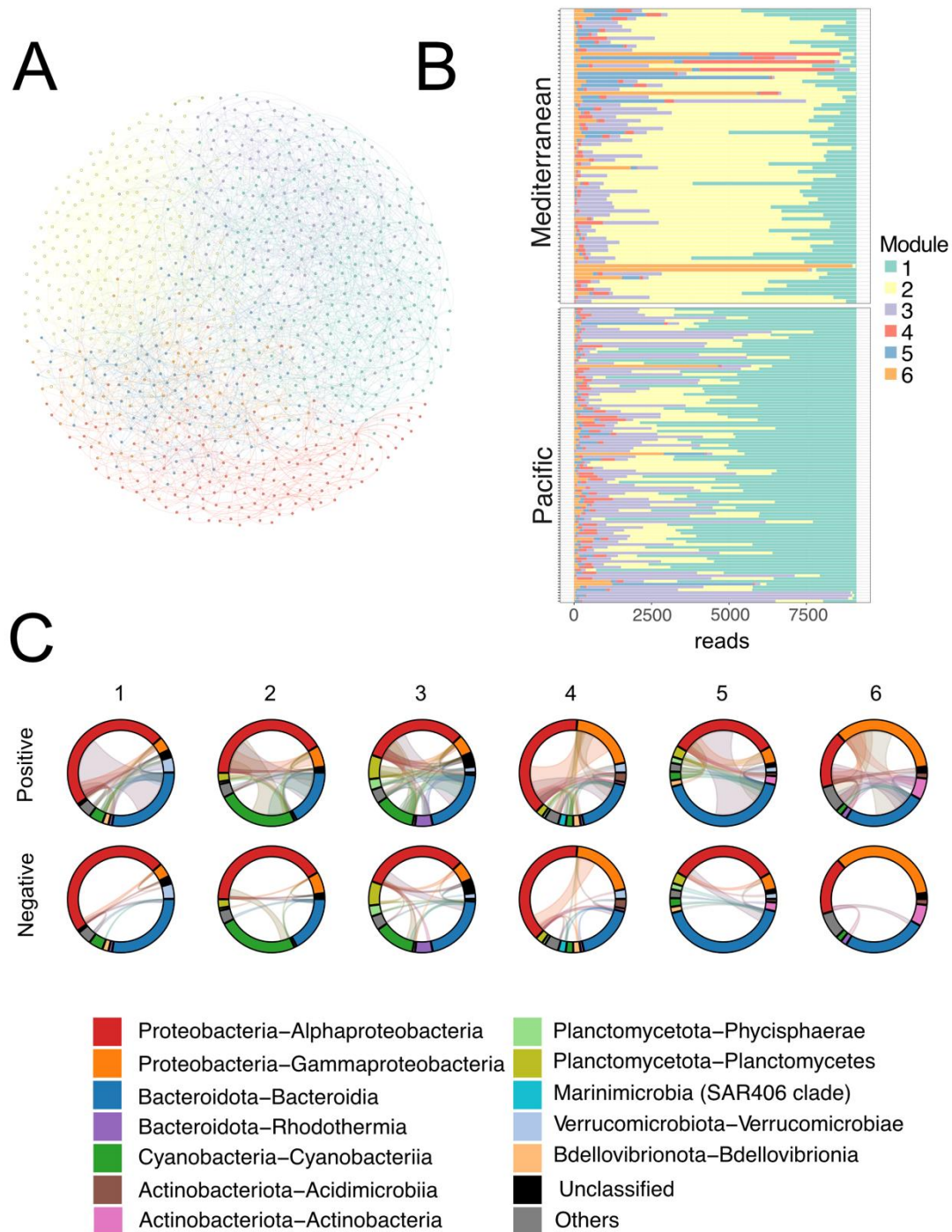
442 A co-occurrence network was inferred using all PMD samples across both oceanic
 443 regions with the goal to identify and delineate potentially shared community network structures.
 444 Although there was a small imbalance in sampling between the Mediterranean Sea (n=114) and
 445 the Pacific Ocean (n=104), the inferring a global PMD network using all PMD samples allowed

446 us to gather more information without affecting ecological interpretations (see supplementary
447 text). Thus, this global network derived using the entire PMD dataset including both ocean
448 regions was used in the following analyses. We decomposed the PMD co-occurrence network
449 into modules using the leading eigenvector algorithm. We identified seven modules (**Fig. 6A**),
450 each representing a distinct community of highly connected OTUs. We considered modules 1
451 to 6 for further analysis, as the module 7 was composed of only 3 OTUs and was thus not
452 relevant in terms of relative abundance.

453 Specific modules presented distinct abundance patterns within Mediterranean and Pacific
454 regions (**Fig. 6B**). Modules 1 and 3 were detected significantly more abundant in the Pacific
455 Ocean, while modules 2 and 6 were more abundant in the Mediterranean Sea. In contrast,
456 modules 4 and 5 did not appear to be driven by geographical provenance. The geographic
457 specificity of these modules highlighted the presence of conserved plastisphere communities in
458 both ocean regions. The module 1 was clearly more related to co-occurring OTUs in PMD
459 samples from the Pacific, while module 2 was more related to co-occurring OTUs in PMD
460 samples from the Mediterranean Sea. The module 3 appeared present in both Pacific and
461 Mediterranean regions, but was significantly enriched in abundance in Pacific samples.

462 The taxonomic distribution of delineated modules (**Fig. 6C**) highlighted a higher
463 prevalence of *Bacteroidota* in module 1 (enriched in Pacific samples), while *Cyanobacteria*
464 were more prevalent in module 2 (enriched in Mediterranean samples). Module 2 (enriched in
465 Mediterranean) and 3 (enriched in Pacific) showed a similar composition and network structure
466 as shown by a detailed analysis of associations between modules (**Suppl. Fig. 2**), indicating a
467 relatively high number of shared co-occurrences between OTUs of both modules. Module
468 composition showed that biogeographic distinct communities associated with PMD articulate
469 around the primary producers *Cyanobacteria* (Module 2 for the Mediterranean Sea and 3 for
470 the Pacific Ocean). Less abundant and less distinct modules showed more diverse taxonomic
471 composition and stronger in-group correlation (**Fig. 6C**). Noteworthy, modules 4-6 showed a
472 contrasting taxonomic structuring, characterized by a low diversity in *Cyanobacteria* OTUs and
473 an increased richness in *Bacteroidota* and *Gammaproteobacteria*.

474



475

476 **Figure 6.** Co-occurrence network in PMD originated from Mediterranean and Pacific regions with (A)

477 module decomposition, (B) distribution of modules per oceanic region and (C) chord diagrams.

478

479 3.8. Metagenome prediction to evaluate the functional redundancy in FL, PA and PMD

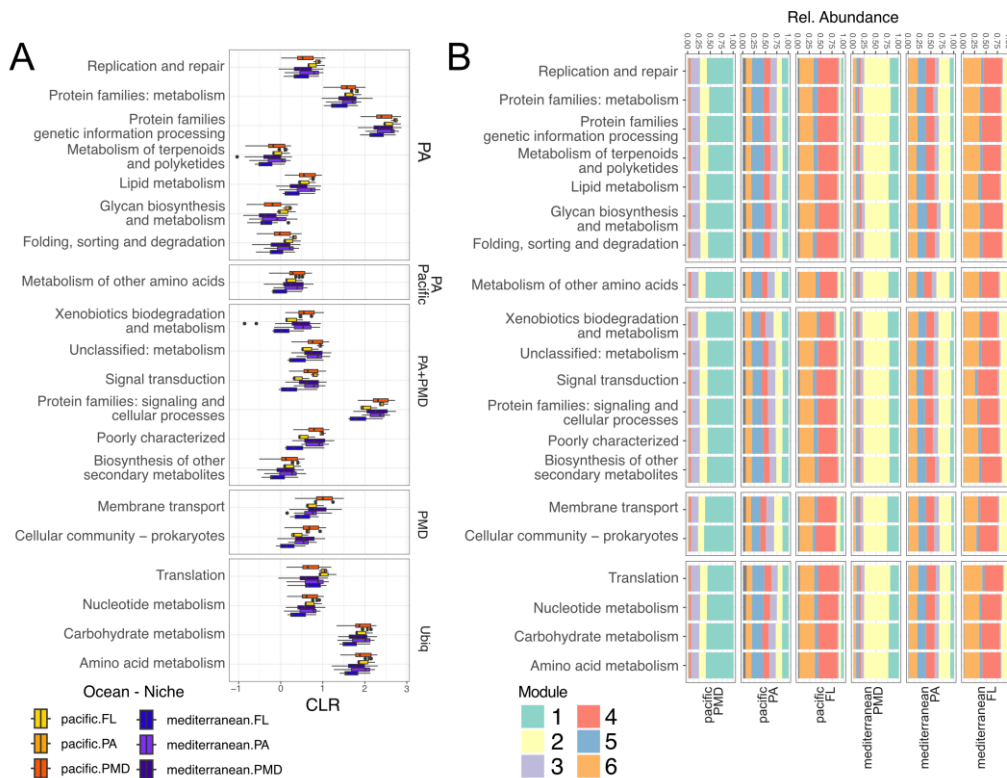
480

481 Analysis of the predicted metabolic capacities encoded by the bacterial communities
 482 associated with FL, PA and PMD lifestyles revealed a number of systematic differences (**Fig.**
 483 **7**). Here, we first identified predicted functions that were prevalent in a combination of ocean-
 niche samples (**Fig. 7A**) to guide the interpretation. For instance, L2 categories “Protein

484 Families: signalin and cellular process” and “Biosynthesis of other secondary metabolites” were
 485 enriched in both PA and PMD, but not in FL (therefore grouped in the PA+PMD subpanel).
 486 “Membrane transport” and “Cellular Community - prokaryotes” functions were abundant in
 487 both Mediterranean-PMD and Pacific-PMD samples, marked as enriched in PMD context.

488 Next, we analyzed the relative contribution of each module to the total predicted
 489 metagenome by ocean-niche, pointing out enriched functions that were driven by the relative
 490 abundance of previously detected community modules in each ocean (Fig. 7B). Despite the
 491 different taxonomic composition of modules, predicted L2 functions were equally enriched in
 492 most cases, thus showing functional redundancy between niche-specific distinct communities.

493 To dig further in specific categories in FL, PA and PMD systems, we calculated the
 494 relative abundance of L3 paths within the selected L2 pathways of Figure 7 (Suppl. Fig. 3).



495
 496 **Figure 7. Metagenome prediction.** (A) CLR transformed abundances for enriched functions per ocean-
 497 niche. Subpanels show combinations of ocean-niche samples where functions show a significantly
 498 higher CLR mean. Subpanel codes: PA= Particle Attached, PA_Pacific = Particle Attached in the
 499 Pacific, PA+PMD = Particle Attached and PMD, PMD = PMD, and Ubiq = Ubiquitous. (B) Relative
 500 abundance of function by module per niche and ocean-niche.

501 **4. Discussion**

502 **4.1. Niche partitioning between FL, PA and PMD lifestyles**

503 The results presented here demonstrated a clear niche partitioning in seasurface
504 prokaryotes at the ocean-basin-scale as reflected in significant differences in the composition
505 of FL, PA and PMD bacterial communities. FL and PA marine microbial communities have
506 repeatedly been shown to differ in their diversity (α -diversity) and composition (β -diversity) in
507 different locations worldwide (Crump et al. 1999; Ghiglione et al. 2005, 2007; Grossart 2010;
508 Ortega-Retuerta 2013). More recently, another type of marine bacterial communities living on
509 PMD was shown to differ from FL (Zettler et al. 2013; Debroas et al. 2017) and also from PA
510 (Dussud et al. 2018a; Oberbeckmann et al. 2018). In this study, we observed that the spatially
511 isolated Western Mediterranean and North Pacific Gyre hosted FL, PA and PMD communities
512 that consistently differed in β -diversity. This result is in accordance with previous studies
513 showing that differences between FL and PA lifestyles exceeded the global-scale geographical
514 variation (Acinas et al. 1997; Salazar et al. 2015). Here, we show that it is not only the case for
515 FL and PA lifestyles, but also for the PMD, which indicates that the strong niche partitioning
516 already observed in different locations (Oberbeckmann et al. 2018; Xu et al. 2019) is confirmed
517 at the ocean-basin-scale.

518

519 **4.2. Ocean-basin-scale comparison revealed a clear influence of environmental 520 parameters on FL, PA and PMD lifestyles**

521 Our ocean-basin-scale comparison showed that the bacterial community structure (β -
522 diversity) within the FL, PA and PMD lifestyles were clearly influenced by their geographical
523 origin, i.e. Mediterranean vs. Pacific regions. This was also visible for α -diversity, with higher
524 Shannon diversity index on FL, PA, and PMD lifestyles in the North Pacific gyre compared to
525 the Western Mediterranean Sea. In particular, we observed a higher selection of given species
526 on PMD in the Pacific (higher richness and lower evenness) compared to the Mediterranean
527 Sea. Our results are in accordance with previous data revealing clear links between
528 environmental variables and global bacterial biogeography of both FL, PA and PMD lifestyles
529 (Ghiglione and Murray 2012; Salazar et al. 2015; Amaral-Zettler et al. 2015).

530 Such biogeographical patterns can result from two ecological processes: (a) the
531 ‘environmental selection’, build on the principle that the existence of environmental difference
532 between basins exert different pressures on each group (FL, PA or PMD) or (b) the ‘dispersal
533 effect’, where the reduced dispersal capabilities of microbes between basins are considered by

534 each lifestyle (Hanson et al. 2012). We estimated the relative contribution of both processes by
535 relating community composition to a set of environmental variables, and to the geographical
536 distance between sampling locations, using multiple regression. First, we found that
537 temperature was the main environmental driver of bacterial communities in all lifestyles, which
538 was in accordance with another study based on *Tara* expeditions on global planktonic ocean
539 microbiome in the epipelagic zone (Sunagawa et al. 2015). On another hand, we observed that
540 the effect of geographical distance was also significant between both ocean basins for the three
541 lifestyles ($p < 0.05$), but not within the same basin. One of the potentially effects of marine debris
542 is that it offers opportunities for the dispersal, or ‘hitchhiking’ of species around the world
543 (Debroas et al. 2017). This may be true on a regional scale, but not at the global Ocean-basin-
544 scale, as shown in our study. We observed a clear distance-decay in all bacterial lifestyles
545 (PMD, FL and PA) that remained relatively close in the same basin (Mediterranean Sea or the
546 North Pacific gyre), but significantly differed at the global Ocean-basin-scale. As a
547 consequence, our results indicate that environmental selection rather than dispersal effects
548 appear to shape the biogeography of the FL, PA and PMD lifestyles at the Ocean-basin-scale,
549 although spurious distance effects may arise as a result of unmeasured environmental variables
550 (Hanson et al. 2012).

551

552 **4.3. Relation between the polymer type and its corresponding plastisphere**

553 In the specific case of PMD, we also evaluated the influence of the polymer composition,
554 morphology, size and age in shaping this specific community. As in many other places in the
555 world surface oceans (Erni-Cassola et al. 2019), PE was the most abundant polymer in both
556 oceanic regions ($> 70\%$), followed by PP, PS together or not with PET in the North Pacific gyre
557 or in the western Mediterranean Sea, respectively. After comparing a total of 179 plastic pieces
558 of different polymer composition, we could not find any significant relation between the
559 bacterial community structure and the polymer type, morphology, size or age. Our study gives
560 another proof that the environmental conditions rather than the polymer characteristics are
561 driving the plastisphere composition at both global (Amaral-Zettler et al. 2015) and regional
562 scales (Dussud et al. 2018a; Basili et al. 2020). This result may appear in contradiction with
563 other studies showing distinct biofilm community structure according to different polymer
564 types (Oberbeckmann et al. 2018; Dussud et al. 2018b; Pinto et al. 2019). Such discrepancy
565 may be explained by the fact that these latter studies were focused on the formation of the
566 biofilm when pristine new plastic were immersed for several weeks or months in seawater,
567 which is different from sampling microplastics directly in the environment that likely stayed

568 longer in seawater. PMD are long-lived substrates that can transport microbial communities
569 across ocean basins. Our results, together with other global comparisons between the North
570 Pacific and North Atlantic gyres (Amaral-Zettler et al. 2015), are indicating that the
571 environmental selection is even more important in shaping the specific community growing on
572 PMD.

573

574 **4.4. Conservative patterns in the FL, PA and PMD in both oceanic regions**

575 Previous studies highlighted the importance of identifying core microbiomes to unravel
576 the ecology of microbial consortia. It has been proposed that these commonly occurring
577 organisms that appear in all assemblages associated with a particular habitat are likely critical
578 to the function of that type of community (Hamad and Knight 2009). Our dataset using ocean-
579 basin-scale comparison was particularly well suited to describe core microbiomes since distinct
580 habitats could be distinguished in both geographical regions according to biological niche
581 spaces, i.e., seawater, organic particles and plastics (FL, PA and PMD lifestyles, respectively).

582 First, we found a classical trend of the FL and PA core microbiomes in the Mediterranean
583 and Pacific regions. The FL lifestyle was dominated by the genus *SAR11* in both oceanic
584 regions, already identified as a highly prevalent group in the world oceans (Dussud et al. 2018b;
585 Basili et al. 2020). Shared presence of *Cyanobacteria* in the two oceanic regions were also
586 identified in the FL core microbiome, being 2.7 times more important in the Mediterranean than
587 in the Pacific. *Cyanobacteria* are generally influenced by water temperature, excess of nitrogen
588 and by the N:P ratio (Dolman et al. 2012). Differences between the two regions resulted in the
589 dominance of *Synechococcus* sp. in the Mediterranean and *Prochlorococcus* sp. in the Pacific,
590 two of the most widespread phototrophic bacterial genera in the oceans (Suzuki et al. 2017;
591 Sunagawa et al. 2020). As depicted elsewhere, the core microbiome in PA samples was
592 characterized by the dominance of *Gammaproteobacteria* and *Alteromonadaceae*. It is well
593 known that *Alteromonas* bacteria have generally higher nutrient requirements than the free-
594 living *SAR11*, and attach to particles to avoid the nutrient-depleted conditions in the surrounding
595 waters (Crespo et al. 2013).

596 Second, we demonstrated that conservative patterns found in PMD communities
597 originated from the two distinct environmentally and geographically distant oceanic regions.
598 We identified a higher number of OTUs shared between both oceanic regions in the PMD (69%
599 of the total OTUs) compared to FL (45%) and PA (49%). Similar results were found in other
600 studies exploring the biogeography of FL marine bacteria worldwide (Salazar et al. 2016,
601 Villarino et al. 2022). Our results confirm again the specificity of the distinct and uniquely PMD

602 habitat at global scale, and suggests that the relative homogeneity of PMD characteristics
603 (composition, morphology, size and age) across the two oceanic regions is a conducive
604 environment for consistent components across the complex plastisphere assemblages. The
605 PMD core microbiome was dominated by *Alphaproteobacteria* (45% of the shared PMD OTUs
606 across the two oceanic regions), *Cyanobacteria* (29%) and *Bacteroidia* (15%).
607 *Rhodobacteraceae* were particularly well represented (25% of the PMD community on average
608 in the two regions) with *Tateyamaria* sp. already isolated in the plastisphere of several regions
609 of the world, such as the North Atlantic, the North Pacific, the North Sea, in estuaries or in the
610 Baltic Sea (Rogers et al. 2020). The *Rhodobacteraceae* has been described as a key taxonomic
611 group in marine biofilm formation, as they were classically found as primary colonizers and the
612 extracellular polymeric substances (EPS) they produce promotes the further attachment of other
613 microorganisms (Dang et al. 2013, Elifantz et al. 2013). It has previously been suggested that
614 these specific bacteria colonizing a virgin plastic surface might have a distinct advantage over
615 other microbial lineages over a given period of time (Zettler et al. 2020). Despite to other
616 taxonomic groups of primo-colonizers that generally do not remain during the different phases
617 of the mature biofilm formation (Odobel et al. 2021), *Rhodobacteraceae* have been repeatedly
618 found in the marine plastisphere (Zettler et al. 2020), thus suggesting that this taxonomic group
619 may remain for longer period of time than other primo-colonizers. It is probably due to the
620 genome plasticity of this taxonomic group that might explain its adaptability and very versatile
621 physiology to dwell in a wide variety of plastic biofilms (Simon et al. 2017). Marine
622 *Rhodobacteraceae* are one of the major subdivisions of *Alphaproteobacteria* and they are
623 highly abundant in the pelagic zone and in algae-associated biofilms, thus playing a crucial role
624 in the cycling of biogeochemical elements (Elifantz et al. 2013). Members of the family
625 *Rhodobacteraceae* are also known to break down hydrocarbons in environmental settings, such
626 as post Deepwater Horizon (Jin et al. 2012). This is not the first study to identify
627 hydrocarbonoclastic bacteria in the plastisphere, a finding which suggests that such group may
628 be involved in the biodegradation of petroleum-based plastics (Zettler et al. 2013). Further
629 studies are needed to evaluate if plastic biodegradation capabilities may be part of the selection
630 processes and community dynamics that influence the fate of plastic-specific bacteria in marine
631 ecosystems.

632 The PMD core microbiome was also dominated by *Cyanobacteria* (13% of the shared
633 PMD OTUs across the two oceanic regions). *Phormidium* and *Rivularia* (mainly *Calothrix* sp.)
634 dominated this photoautotrophic group, as previously found in other plastisphere communities
635 (Zettler et al. 2013; Bryant et al. 2016; Dussud et al. 2018a). Such finding is of great interest

636 according to the recent demonstration of high autotrophic activity on plastics, which can
637 support the bacterial carbon demand needed for heterotrophic activities (net autotrophy)
638 (Bryant et al. 2016). These results confirm the potential role played by the plastisphere in the
639 biogeochemical cycles in the context of an increasing number of plastic particles in the marine
640 environment (Conan et al. 2022). Interestingly, we also found almost 17% of potentially
641 hydrocarbonoclastic bacteria in the PMD core microbiome, including well-known linear or
642 branched hydrocarbon degraders such as *Alcalinovorax* sp. and *Marinobacter* sp. (Gutierrez
643 2019). However, similar percentages were also found in FL and PA core microbiome,
644 underlining their ubiquitous presence in our samples. This was also the case for putative
645 pathogens, even if OTUs belong to *Vibrio* sp. (including *V. parahaemolyticus*, *V. anguillarum*,
646 *V. harveyi*, *V. pectinida*, *V. xiamenensis*) were 3 to 32 times higher on PMD compared to FL
647 and PA in both regions. Mechanism for the persistence and spread of potential pathogens such
648 as *Vibrio* bacteria remain unknown (Amaral-Zettler et al. 2015). Because the metabarcoding
649 approach is not an appropriate method for describing bacterial virulence, more in-depth studies
650 are needed to assess the pathogenicity of the OTUs identified in this study.

651

652 **4.5. Ocean-specific PMD communities identified through co-occurrence network analysis**

653 With the goal to identify PMD-specific communities, we inferred a cross-ocean co-
654 occurrence network of OTUs from PMD samples. The analysis of this network using a
655 community detection algorithm revealed communities specifically associated to plastic
656 particles in both the Pacific Ocean and the Mediterranean Sea. While a specific community was
657 identified as enriched in abundance in the Pacific samples (Module 1), distinct from the
658 community enriched Mediterranean samples (Module 2), both these communities (or modules)
659 were detected in all PMD samples and harbored similar functional potential with specific
660 enriched predicted functions (as discussed below). A specific signature of Module 1 (Pacific
661 enriched) was the higher prevalence of associations between *Alphaproteobacteria* and
662 *Bacteroida*, while Module 2 (Mediterranean enriched) had a distinctive signature with a specific
663 enrichment of associations between *Cyanobacteria* and *Alphaproteobacteria* as well as
664 *Bacteroida*. These results confirm previous observation of the importance of *Cyanobacteria* in
665 the plastisphere bacterial communities classically found in the Mediterranean Sea (Dussud et
666 al. 2018, Zettler et al. 2021). Nitrogen-fixing cyanobacteria are playing key roles in the primary
667 production of organic matter, especially in an oligotrophic environment like the Mediterranean
668 Sea (Le Moal and Biegala 2009; Uysal and Koksalan 2006). A recent study underlined the
669 strong relationships between microbial activities in the Mediterranean plastisphere by primary

670 producers and heterotrophic bacteria (Conan et al. 2022). This type of relationship might
671 explain the co-occurrence of both autotrophic *Cyanobacteria* and heterotrophic
672 *Alphaproteobacteria* and *Bacteroida* found in the Module 1. Causal effect between
673 *Cyanobacteria* and eukaryotic dinoflagellates was also previously demonstrated in the
674 plastisphere from the Mediterranean Sea, a pairing that may be related to nitrogen-fixing
675 capacity in the cyanobacterium in oligotrophic environment (Zettler et al. 2021). Overall, this
676 cross-ocean co-occurrence network analysis thus revealed the relative contribution of specific
677 PMD-specific communities across samples, but also likely underlined the need for further
678 studies to better understand the importance of co-occurrence associations in the role of the
679 plastisphere in global biogeochemical cycles.

680

681 **4.6. Functional potential and redundancy in PMD compared to FL, PA lifestyles in both** 682 **oceanic regions**

683 Finally, we explore the functional redundancy of the plastisphere in comparison to FL
684 and PA lifestyles in the two oceanic regions. Functional redundancy has been approached by
685 prediction of microbial metagenomes in FL or PA against PMD lifestyles and across the two
686 oceanic regions. PICRUST analysis highlighted the dominance of a set of putative functions on
687 PMD compared to FL and PA lifestyles. Although these comparisons were based purely on
688 predictions made from 16S rRNA gene sequences (Langille et al. 2013; Louca et al. 2016), we
689 found that several important function in the carbon biogeochemical cycle, biofilm formation,
690 microbial turnover and nutrient efficiency were overrepresented functional categories on PMD
691 compared to FL and PA. The dominance of photosynthesis and heterotrophic metabolism
692 (carbohydrate metabolism, amino acid, vitamin metabolism) on PMD are consistent with the
693 role played by the plastisphere in the biogeochemical cycles in the context of an increasing
694 number of plastic particles in the marine environment (Bryant et al. 2016). Another prediction
695 of overrepresented functional categories on PMD compared to FL and PA was also plausible:
696 the membrane transport functions and the ABC transporters, as well as the cellular processes
697 and signal transduction were previously described as essential functions in biofilm formation
698 and maturation (Lasa and Penadés 2006; Porter et al. 2011; He and Bauer 2014). Other
699 metabolic pathways, including nitrogen and sulfur metabolism were also enhanced in PMD,
700 which is in accordance with recent findings showing that microbial turnover and nutrient
701 efficiency was enhanced in the plastisphere (Zhou et al. 2021). These all suggested that
702 plastisphere communities could participate in a large number of important ecological processes

703 in the marine ecosystem (Bhagwat et al. 2021). Interestingly, our study does not put into
704 evidence the enhanced metabolic pathways belonging to xenobiotics biodegradation in the
705 plastisphere, as compared to FL and PA lifestyles. Previous studies underlined the presence of
706 various contaminants sorbed on PMD surface, including persistent organic pollutants (POPs)
707 and heavy metals (Alimba and Faggio 2019). We also observed the presence of putative
708 xenobiotic degradation genes on PMD, as well as the conservative presence of well-known
709 linear or branched hydrocarbon degraders such as *Alcalinovorax* sp. and *Marinobacter* sp.
710 (Sekiguchi et al. 2011). However, our study suggests that the plastisphere does not suffer from
711 more environmental stress compared to the surrounding seawater.

712

713 **5. Conclusion**

714 The clear niche partitioning together with the description of a core microbiome that could
715 be characterized at the ocean-basin-scale have important implications for understanding
716 microbial interactions with plastic on a global scale. Autotrophic and heterotrophic organisms
717 were always found on PMD in the two oceanic regions, thus reinforcing the importance of
718 future studies exploring the relative importance of the plastisphere on the carbon sink
719 (absorbing carbon dioxide from the atmosphere) or source in the Ocean. Our functional
720 predictive analysis also revealed the importance of nitrogen and sulfur metabolisms on
721 microplastics that open new questions on the role of the plastisphere in a large number of
722 important ecological processes in the marine ecosystem. Finally, our finding that Pacific and
723 Mediterranean plastisphere communities are distinct from each other allowed us to statistically
724 prove the importance of environmental selection, rather than polymer type or dispersal effects,
725 in driving changes in plastisphere communities at the Ocean-basin-scale. It opens new routes
726 for further studies on our ability to predict the plastisphere community responses to
727 environmental changes.

728

729 **Acknowledgments**

730 We thank the commitment of the following institutions, persons and sponsors: CNRS,
731 EMBL, CEA, and other organizations: the Tara Ocean Foundation teams and crew, its sponsors
732 and partners agnès b., Prince Albert II of Monaco, Veolia Foundation, Bic, Compagnie
733 Nationale du Rhône, L'Oréal, Biotherm, Région Bretagne, Lorient Agglomération, Région
734 Aquitaine, Région Sud, Billerudkorsnas, Office Français de la Biodiversité, Etienne Bourgois,
735 the "Tara" schooner and crew. We are also grateful to the French Ministry of Foreign Affairs
736 for supporting the Tara expedition. We are grateful to Guigui PA, VF, JS, JP for insightful

737 comments on the manuscript.

738

739

740 **References**

741

742 Acinas SG, Rodríguez-Valera F, Pedrós-Alió C (1997) Spatial and temporal variation in marine
743 bacterioplankton diversity as shown by RFLP fingerprinting of PCR amplified 16S rDNA.
744 FEMS Microbiol Ecol 24: 27–40. <https://doi.org/10.1111/j.1574-6941.1997.tb00420.x>

745 Aguila-Torres P, González M, Maldonado JE, Miranda R, Zhang L, González-Stegmaier R,
746 Rojas LA, Gaete A (2022). Associations between bacterial communities and microplastics from
747 surface seawater of the Northern Patagonian area of Chile. Environ Poll, 306, 119313.
748 <https://doi.org/10.1016/j.envpol.2022.119313>

749 Alimba CG, Faggio C (2019) Microplastics in the marine environment: current trends in
750 environmental pollution and mechanisms of toxicological profile. Environ Tox Pharmacol 68:
751 61–74. <https://doi.org/10.1016/j.etap.2019.03.001>

752 Amaral-Zettler LA, Zettler ER, Mincer TJ (2020) Ecology of the plastisphere. Nat Rev
753 Microbiol 18: 139–151. <https://doi.org/10.1038/s41579-019-0308-0>

754 Amaral-Zettler LA, Zettler ER, Slikas B, Boyd GD, Melvin DW, Morrall CE, et al (2015) The
755 biogeography of the plastisphere: implications for policy. Front Ecol Env 13: 541–546.
756 <https://doi.org/10.1890/150017>

757 Anderson DG, McKay LL (1983) Simple and rapid method for isolating large plasmid DNA
758 from lactic streptococci. Appl Environ Microbiol 46:549–52.
759 <https://doi.org/10.1128/aem.46.3.549-552.1983>

760 Bandinelli SC, Fuggetta A, Ghezzi C (1993) Software process model evolution in the SPADE
761 environment. IEEE transactions on software engineering 19: 1128-1144.

762 Basili M, Quero GM, Giovannelli D, Manini E, Vignaroli C, Avio CG, et al (2020) Major role
763 of surrounding environment in shaping biofilm community composition on marine plastic
764 debris. Front Mar Sci 7. <https://doi.org/10.3389/fmars.2020.00262>

765 Bhagwat G, Zhu Q, O'Connor W, Subashchandrabose S, Grainge I, Knight R, et al (2021)
766 Exploring the composition and functions of plastic microbiome using whole-genome
767 sequencing. *Environ Sci Technol* 55: 4899–4913. <https://doi.org/10.1021/acs.est.0c07952>

768 Bryant JA, Clemente TM, Viviani DA, Fong AA, Thomas KA, Kemp P, et al (2016) Diversity
769 and activity of communities inhabiting plastic debris in the north pacific gyre. *mSystems* 1.
770 <https://doi.org/10.1128/msystems.00024-16>

771 Camacho C, Coulouris G, Avagyan V, Ma N, Papadopoulos J, Bealer K, et al (2009) BLAST+:
772 architecture and applications. *BMC Bioinformatics* 10: 421. [https://doi.org/10.1186/1471-](https://doi.org/10.1186/1471-2105-10-421)
773 [2105-10-421](https://doi.org/10.1186/1471-2105-10-421)

774 Chen X, Chen X, Zhao Y, Zhou H, Xiong X, Wu C (2020) Effects of microplastic biofilms on
775 nutrient cycling in simulated freshwater systems. *Sci Total Environ* 719: 137276.
776 <https://doi.org/10.1016/j.scitotenv.2020.137276>

777 Cheng J, Jacquin J, Conan P, Pujo-Pay M, Barbe V, George M, et al (2020) Relative influence
778 of plastic debris size and shape, chemical composition and phytoplankton-bacteria interactions
779 in driving seawater plastisphere abundance, diversity and activity. *Front Microbiol* 11: 610231.
780 [https://doi.org/10.3389/fmicb.\(2020\).610231](https://doi.org/10.3389/fmicb.(2020).610231)

781 Clarke KR, Warwick RW (2001) Change in marine communities: an approach to statistical
782 analysis and interpretation, 2nd edition, Primer-E: Plymouth.

783 Clauset A, Newman MEJ, Moore C (2004) Finding community structure in very large networks.
784 *Phys Rev E* 70: 066111. <https://doi.org/10.1103/PhysRevE.70.066111>

785 Conan P, Philip L, Ortega-Retuerta E, Odobel C, Duran C, Pandin C, Giraud C, Meistertzheim
786 AL, Barbe V, Ter Hall A, Pujo-Pay M, Ghiglione JF (2022) Evidence of coupled autotrophy
787 and heterotrophy on plastic biofilms and its influence on surrounding seawater. *Environ Pollut.*
788 315:120463. <https://doi.org/10.1016/j.envpol.2022.120463>.

789 Cozar A, Echevarria F, Gonzalez-Gordillo JJ, Irigoien X, Ubeda B, Hernandez-Leon S, et al
790 (2014) Plastic debris in the open ocean. *Proceedings of the National Academy of Sciences* 111:
791 10239–10244. <https://doi.org/10.1073/pnas.131470511>

792 Crespo BG, Pommier T, Fernández-Gómez B, Pedrós-Alió C (2013) Taxonomic composition
793 of the particle-attached and free-living bacterial assemblages in the Northwest Mediterranean
794 Sea analyzed by pyrosequencing of the 16S rRNA. *Microbiologyopen* 2: 541–552.
795 <https://doi.org/10.1002/mbo3.92>

796 Crump BC, Armbrust EV, Baross JA (1999) Phylogenetic analysis of particle-attached and free-
797 living bacterial communities in the columbia river, its estuary, and the adjacent coastal ocean.
798 *Appl Environ Microbiol* 65: 3192–3204. <https://doi.org/10.1128/AEM.65.7.3192-3204.1999>

799 Dang H, Li T, Chen M, Huang G (2008) Cross-ocean distribution of *Rhodobacterales* bacteria
800 as primary surface colonizers in temperate coastal marine waters. *Appl Environ Microbiol* 74:
801 52–60. <https://doi.org/10.1128/AEM.01400-07>.

802 Debroas D, Mone A, Ter Halle A (2017) Plastics in the North Atlantic garbage patch: a boat-
803 microbe for hitchhikers and plastic degraders. *Sci Total Environ* 599–600: 1222–1232.
804 <https://doi.org/10.1016/j.scitotenv.2017.05.059>

805 Dolman A, Rucker J, Pick F, Fastner J, Rohrlack T, Mischke U, et al (2012) Cyanobacteria and
806 cyanotoxins: the influence of nitrogen versus phosphorus. *PloS one* 7: e38757.
807 <https://doi.org/10.1371/journal.pone.0038757>

808 Douglas GM, Maffei VJ, Zaneveld JR et al (2020) PICRUSt2 for prediction of metagenome
809 functions. *Nat Biotechnol* 38: 685–688. <https://doi.org/10.1038/s41587-020-0548-6>

810 Dussud C, Hudec C, George M, Fabre P, Higgs P, Bruzaud S, et al (2018b) colonization of non-
811 biodegradable and biodegradable plastics by marine microorganisms. *Front Microbiol* 9.

812 Dussud C, Meistertzheim AL, Conan P, Pujo-Pay M, George M, Fabre P, et al (2018a) Evidence
813 of niche partitioning among bacteria living on plastics, organic particles and surrounding
814 seawaters. *Environmental Pollution* 236: 807–816.
815 <https://doi.org/10.1016/j.envpol.2017.12.027>

816 Elifantz H, Horn G, Ayon M, Cohen Y, Minz D (2013) *Rhodobacteraceae* are the key members
817 of the microbial community of the initial biofilm formed in Eastern Mediterranean coastal
818 seawater. *FEMS Microbiol Ecol* 85: 348–357. <https://doi.org/10.1111/1574-6941.12122>

819 Erni-Cassola G, Zadjelovic V, Gibson MI, Christie-Oleza JA (2019) Distribution of plastic
820 polymer types in the marine environment: a meta-analysis. *Journal of Hazardous Materials* 369:
821 691–698. <https://doi.org/10.1016/j.jhazmat.2019.02.067>

822 Escudié F, Auer L, Bernard M, Mariadassou M, Cauquil L, Vidal K, et al (2018) FROGS: find,
823 rapidly, otus with galaxy solution. *Bioinformatics* 34: 1287–1294.
824 <https://doi.org/10.1093/bioinformatics/btx791>

825 Ghiglione J-F, Larcher M, Lebaron P (2005) Spatial and temporal scales of variation in
826 bacterioplankton community structure in the NW Mediterranean Sea. *Aquatic Microbial*
827 *Ecology* 40: 229–240. <https://doi.org/10.3354/ame040229>

828 Ghiglione J-F, Laudet V (2020) marine life cycle: a polluted terra incognita is unveiled. *Curr*
829 *Biol* 30: R130–R133. <https://doi.org/10.1016/j.cub.2019.11.083>

830 Ghiglione JF, Mevel G, Pujo-Pay M, Mousseau L, Lebaron P, Goutx M (2007) Diel and
831 seasonal variations in abundance, activity, and community structure of particle-attached and
832 free-living bacteria in nw mediterranean sea. *Microb Ecol* 54: 217–231.
833 <https://doi.org/10.1007/s00248-006-9189-7>

834 Ghiglione JF, Murray AE (2012) Pronounced summer to winter differences and higher
835 wintertime richness in coastal Antarctic marine bacterioplankton. *Environmental Microbiology*
836 14: 617–629. <https://doi.org/10.1111/j.1462-2920.2011.02601.x>

837 Ghiglione JF, Palacios C, Marty JC, Mével G, Labruno C, Conan P, et al (2008) Role of
838 environmental factors for the vertical distribution (0–1000 m) of marine bacterial communities
839 in the NW Mediterranean Sea. *Biogeosciences* 5: 1751–1764. [https://doi.org/10.5194/bg-5-](https://doi.org/10.5194/bg-5-1751-2008)
840 1751-2008

841 Grossart HP (2010) Ecological consequences of bacterioplankton lifestyles: changes in
842 concepts are needed. *Environmental Microbiology Reports* 2: 706–714.
843 <https://doi.org/10.1111/j.1758-2229.2010.00179.x>

844 Gutierrez T (2019) Occurrence and roles of the obligate hydrocarbonoclastic bacteria in the
845 ocean when there is no obvious hydrocarbon contamination. In: McGenity TJ (ed). *Taxonomy,*
846 *Genomics and Ecophysiology of Hydrocarbon-Degrading Microbes*. Springer International
847 Publishing, Cham, pp 337–352. https://doi.org/10.1007/978-3-319-60053-6_14-1

848 Hamady M, Knight R (2009) Microbial community profiling for human microbiome projects:
849 Tools, techniques, and challenges. *Genome Res* 19: 1141–1152.
850 <https://doi.org/10.1101/gr.085464.108>

851 Hanson CA, Fuhrman JA, Horner-Devine MC, Martiny JBH (2012) Beyond biogeographic
852 patterns: processes shaping the microbial landscape. *Nature Reviews Microbiology* 10: 497–
853 506. <https://doi.org/10.1038/nrmicro2795>

854 He K, Bauer CE (2014) Chemosensory signaling systems that control bacterial survival. *Trends*
855 *in Microbiology* 22: 389–398. <https://doi.org/10.1016/j.tim.2014.04.004>

856 Isobe A, Azuma T, Cordova MR, Cózar A, Galgani F, Hagita R, et al (2021) A multilevel
857 dataset of microplastic abundance in the world’s upper ocean and the Laurentian Great Lakes.
858 *Microplastics and Nanoplastics 1*: 1-14. <https://doi.org/10.1186/s43591-021-00013-z>

859 Jacquin J, Cheng J, Odobel C, Pandin C, Conan P, Pujo-Pay M, et al (2019) microbial
860 ecotoxicology of marine plastic debris: a review on colonization and biodegradation by the
861 “plastisphere”. *Front Microbiol* 10. <https://doi.org/10.3389/fmicb.2019.00865>

862 Jin HM, Kim JM, Lee HJ, Madsen EL, Jeon CO (2012) *Alteromonas* as a key agent of
863 polycyclic aromatic hydrocarbon biodegradation in crude oil-contaminated coastal sediment.
864 *Environ Sc Tech* 46: 7731-7740. <https://doi.org/10.1021/es3018545>

865 Kaandorp ML, Lobelle D, Kehl, C, Dijkstra HA, van Sebille E (2023) Global mass of buoyant
866 marine plastics dominated by large long-lived debris. *Nature Geoscience* 16(8): 689-694.
867 <https://doi.org/10.1038/s41561-023-01216-0>

868 Kane IA, Clare MA, Miramontes E, Wogelius R, Rothwell JJ, Garreau P, et al (2020) Seafloor
869 microplastic hotspots controlled by deep-sea circulation. *Science* 368: 1140–1145.
870 <https://doi.org/10.1126/science.aba5899>

871 Kedzierski M, Falcou-Préfol M, Kerros ME, Henry M, Pedrotti ML, Bruzaud S (2019) A
872 machine learning algorithm for high throughput identification of FTIR spectra: application on
873 microplastics collected in the Mediterranean Sea. *Chemosphere* 234: 242–251.
874 <https://doi.org/10.1016/j.chemosphere.2019.05.113>

875 Kirstein IV, Wichels A, Krohne G, Gerdt G (2018) Mature biofilm communities on synthetic
876 polymers in seawater: specific or general? *Marine Environmental Research* 142: 147–154.
877 <https://doi.org/10.1016/j.marenvres.2018.09.028>

878 Kooi M, Nes EH van, Scheffer M, Koelmans AA (2017) Ups and downs in the ocean: effects
879 of biofouling on vertical transport of microplastics. *Environ Sci Technol* 51: 7963–7971.
880 <https://doi.org/10.1021/acs.est.6b04702>

881 Langille MGI, Zaneveld J, Caporaso JG, McDonald D, Knights D, Reyes JA, et al (2013)
882 Predictive functional profiling of microbial communities using 16S rRNA marker gene
883 sequences. *Nat Biotechnol* 31: 814–821. <https://doi.org/10.1038/nbt.2676>

884 Lasa I, Penadés JR (2006) Bap A family of surface proteins involved in biofilm formation.
885 *Research in Microbiology* 157: 99–107. <https://doi.org/10.1016/j.resmic.2005.11.003>

886 Le Moal M, Biegala IC (2009). Diazotrophic unicellular cyanobacteria in the northwestern
887 Mediterranean Sea: a seasonal cycle. *Limnology and oceanography* 54(3), 845-855.
888 <https://doi.org/10.4319/lo.2009.54.3.0845>

889 Lebreton L, Slat B, Ferrari F, Sainte-Rose B, Aitken J, Marthouse R, et al (2018) Evidence that
890 the Great Pacific Garbage Patch is rapidly accumulating plastic. *Scientific Reports* 8: 4666.
891 <https://doi.org/10.1038/s41598-018-22939-w>

892 Louca S, Parfrey LW, Doebeli M (2016) Decoupling function and taxonomy in the global ocean
893 microbiome. *Science* 353: 1272–1277. <https://doi.org/10.1126/science.aaf4507>

894 Mahé F, Rognes T, Quince C, de Vargas C, Dunthorn M (2014) Swarm: robust and fast
895 clustering method for amplicon-based studies. *PeerJ* 2: e593. <https://doi.org/10.7717/peerj.593>

896 Miralles L, Gomez-Agenjo M, Rayon-Viña F, Gyraitè G, Garcia-Vazquez E (2018) Alert
897 calling in port areas: marine litter as possible secondary dispersal vector for hitchhiking
898 invasive species. *Journal for Nature Conservation* 42: 12–18.
899 <https://doi.org/10.1016/j.jnc.2018.01.005>

900 Nava V, Leoni B (2021) A critical review of interactions between microplastics, microalgae
901 and aquatic ecosystem function. *Water Research* 188: 116476.
902 <https://doi.org/10.1016/j.watres.2020.116476>

903 Newman MEJ (2006) Modularity and community structure in networks. Proceedings of the
904 National Academy of Sciences 103 (23): 8577-8582.
905 <https://www.pnas.org/doi/10.1073/pnas.0601602103>

906 Oberbeckmann S, Kreikemeyer B, Labrenz M 2018 Environmental factors support the
907 formation of specific bacterial assemblages on microplastics. Front Microbiol 8.
908 <https://doi.org/10.3389/fmicb.2017.02709>

909 Odobel C, Dussud C, Philip L, Derippe G, Lauters M, Eyheraguibel B, Burgaud G, Ter Halle
910 A, Meistertzheim AL, Bruzard S, Barbe V, Ghiglione JF (2021) Bacterial abundance, diversity
911 and activity during long term colonization of non-biodegradable and biodegradable plastics in
912 seawater. Frontiers in microbiology 12:734782. <https://doi.org/10.3389/fmicb.2021.734782>

913 Ogonowski M, Motiei A, Ininbergs K, Hell E, Gerdes Z, Udekwu KI, et al (2018) Evidence for
914 selective bacterial community structuring on microplastics. Environ Microbiol 20: 2796–2808.
915 <https://doi.org/10.1111/1462-2920.14120>

916 Oksanen J, Blanchet FG, Kindt R, Legendre P, Minchin P, O’Hara B, et al (2015) Vegan:
917 community ecology package. R Package Version 22-1 2: 1–2.

918 Ortega-Retuerta E, Joux F, Jeffrey WH, Ghiglione JF (2013) Spatial variability of particle-
919 attached and free-living bacterial diversity in surface waters from the Mackenzie River to the
920 Beaufort Sea (Canadian Arctic). Biogeosciences 10 (4): 2747-2759. [https://doi.org/10.5194/bg-](https://doi.org/10.5194/bg-10-2747-2013)
921 [10-2747-2013](https://doi.org/10.5194/bg-10-2747-2013)

922 Parada AE, Needham DM, Fuhrman JA (2016) Every base matters: assessing small subunit
923 rRNA primers for marine microbiomes with mock communities, time series and global field
924 samples. Environmental Microbiology 18: 1403–1414. [https://doi.org/10.1111/1462-](https://doi.org/10.1111/1462-2920.13023)
925 [2920.13023](https://doi.org/10.1111/1462-2920.13023)

926 Pedrotti, ML, de Figueiredo Lacerda AL, Petit S, Ghiglione JF, Gorsky G (2022). *Vibrio* spp
927 and other potential pathogenic bacteria associated to microfibers in the North-Western
928 Mediterranean Sea. Plos one, 17: e0275284. <https://doi.org/10.1371/journal.pone.0275284>

929 Pinto M, Langer TM, Hüffer T, Hofmann T, Herndl GJ (2019) The composition of bacterial
930 communities associated with plastic biofilms differs between different polymers and stages of
931 biofilm succession. PLOS ONE 14: e0217165. <https://doi.org/10.1371/journal.pone.0217165>

932 Porter SL, Wadhams GH, Armitage JP (2011) Signal processing in complex chemotaxis
933 pathways. *Nature reviews Microbiology* 9: 153–165. <https://doi.org/10.1038/nrmicro2505>

934 Quast C, Pruesse E, Yilmaz P, Gerken J, Schweer T, Yarza P, et al (2013) The SILVA ribosomal
935 RNA gene database project: improved data processing and web-based tools. *Nucleic Acids Res*
936 41: D590–D596. <https://doi.org/10.1093/nar/gks1219>

937 Rogers K, Carreres-Calabuig JA, Gorokhova E, Posth N (2020) Micro-by-micro interactions:
938 how microorganisms influence the fate of marine microplastics. *Limnology and Oceanography*
939 *Letters* 5. <https://doi.org/10.1002/lol2.10136>

940 Rognes T, Flouri T, Nichols B, Quince C, Mahé F (2016) VSEARCH: a versatile open source
941 tool for metagenomics. *PeerJ* 4: e2584. <https://doi.org/10.7717/peerj.2584>

942 Rummel CD, Jahnke A, Gorokhova E, Kühnel D, Schmitt-Jansen M (2017) Impacts of biofilm
943 formation on the fate and potential effects of microplastic in the aquatic environment. *Environ*
944 *Sci Technol Lett* 4: 258–267. <https://doi.org/10.1021/acs.estlett.7b00164>

945 Salazar G, Cornejo-Castillo FM, Borrull E, Díez-Vives C, Lara E, Vaqué D, et al (2015)
946 Particle-association lifestyle is a phylogenetically conserved trait in bathypelagic prokaryotes.
947 *Mol Ecol* 24: 5692–5706. <https://doi.org/10.1111/mec.13419>

948 Sekiguchi T, Sato T, Enoki M, Kanehiro H, Uematsu K, Kato C (2011) Isolation and
949 characterization of biodegradable plastic degrading bacteria from deep-sea environments.
950 *JAMSTEC Report of Research and Development* 11: 33–41.
951 <https://doi.org/10.5918/jamstecr.11.33>

952 Simon M, Scheuner C, Meier-Kolthoff JP, Brinkhoff T, Wagner-Döbler I, Ulbrich M, Hans-
953 Peter Klenk HP, Schomburg D, Petersen J, Göker M (2017) Phylogenomics of
954 *Rhodobacteraceae* reveals evolutionary adaptation to marine and non-marine habitats. *The*
955 *ISME journal* 11:1483-1499. <https://doi.org/10.1038/ismej.2016.198>

956 Sunagawa S, Acinas SG, Bork P, Bowler C, Eveillard D, Gorsky G, et al (2020) Tara Oceans:
957 towards global ocean ecosystems biology. *Nat Rev Microbiol* 18: 428–445.
958 <https://doi.org/10.1038/s41579-020-0364-5>

959 Sunagawa S, Coelho LP, Chaffron S, Kultima JR, Labadie K, Salazar G, et al (2015) Structure
960 and function of the global ocean microbiome. *Science* 348.
961 <https://doi.org/10.1126/science.1261359>

962 Suzuki S, Kaneko R, Kodama T, Hashihama F, Suwa S, Tanita I, et al (2017) Comparison of
963 community structures between particle-associated and free-living prokaryotes in tropical and
964 subtropical Pacific Ocean surface waters. *J Oceanogr* 73: 383–395.
965 <https://doi.org/10.1007/s10872-016-0410-0>

966 Tackmann J, Matias Rodrigues JF, von Mering C (2019) Rapid inference of direct interactions
967 in large-scale ecological networks from heterogeneous microbial sequencing data. *Cell Systems*
968 9: 286–296.e8. <https://doi.org/10.1016/j.cels.2019.08.002>

969 ter Halle A, Ladirat L, Gendre X, Goudouneche D, Pusineri C, Routaboul C, et al (2016)
970 Understanding the fragmentation pattern of marine plastic debris. *Environ Sci Technol* 50:
971 5668–5675. <https://doi.org/10.1021/acs.est.6b00594>

972 Uysal Z, Koksalan I (2006) The annual cycle of *Synechococcus* (cyanobacteria) in the northern
973 Levantine Basin shelf waters (Eastern Mediterranean). *Marine Ecology* 27 (3): 187–197.
974 <https://doi.org/10.1111/j.1439-0485.2006.00105.x>

975 Villarino E, Watson JR, Chust G, Woodill AJ, Klempay B, Jonsson B, Gasol JM, Logares R,
976 Massana R, Giner CR, Salazar G, Alvarez-Salgado XA, Catala TS, Duarte CM, Agusti S,
977 Mauro F, Irigoien X, Barton AD (2022). Global beta diversity patterns of microbial
978 communities in the surface and deep ocean. *Global Ecology and Biogeography* 31: 2323–2336.
979 <https://doi.org/10.1111/geb.13572>

980 Vroom RJE, Koelmans AA, Besseling E, Halsband C (2017) Aging of microplastics promotes
981 their ingestion by marine zooplankton. *Environmental Pollution* 231: 987–996.
982 <https://doi.org/10.1016/j.envpol.2017.08.088>

983 Xu X, Wang S, Gao F, Li J, Zheng L, Sun C, et al (2019) Marine microplastic-associated
984 bacterial community succession in response to geography, exposure time, and plastic type in
985 China's coastal seawaters. *Marine Pollution Bulletin* 145: 278–286.
986 <https://doi.org/10.1016/j.marpolbul.2019.05.036>

- 987 Zalasiewicz J, Waters CN, Ivar do Sul JA, Corcoran PL, Barnosky AD, Cearreta A, et al. (2016)
988 The geological cycle of plastics and their use as a stratigraphic indicator of the Anthropocene.
989 *Anthropocene* 13: 4–17. <https://doi.org/10.1016/j.ancene.2016.01.002>
- 990 Zettler ER, Mincer TJ, Amaral-Zettler LA (2013) Life in the “plastisphere”: microbial
991 communities on plastic marine debris. *Environmental Science & Technology* 47: 7137–7146.
992 <https://doi.org/10.1021/es401288x>
- 993 Zhao S, Zettler ER, Amaral-Zettler LA, Mincer TJ (2021) Microbial carrying capacity and
994 carbon biomass of plastic marine debris. *The ISME journal* 15: 67-77.
995 <https://doi.org/10.1038/s41396-020-00756-2>
- 996 Zhou J, Gui H, Banfield CC, Wen Y, Zang H, Dippold MA, et al (2021) The microplastisphere:
997 biodegradable microplastics addition alters soil microbial community structure and function.
998 *Soil Biology and Biochemistry* 156: 108211. <https://doi.org/10.1016/j.soilbio.2021.108211>

999 **Declarations**

1000 **-Ethical Approval:** This article follows the Committee on Publication Ethics (COPE)
1001 guidelines. including the ethical responsibilities of the authors. The authors declare that they
1002 obtained study-specific approval from the appropriate ethics committee for the research
1003 content of this article.

1004 **-Consent to Participate:** All the authors agreed to participate in coauthorship. The
1005 authors have no competing interests to declare that they are relevant to the content of this
1006 article.

1007 **-Consent to Publish:** All the coauthors agreed with the content of this article, and they
1008 all provided explicit consent for submission. The authors obtained consent from the
1009 responsible authorities at the institute/organization where the work was carried out before the
1010 work was submitted.

1011 **-Author Contributions (CRediT taxonomy):** **Justine Jacquin:** Formal analysis,
1012 Investigation, Methodology, Visualization, Writing - Original Draft, **Marko Budinich:** Formal
1013 analysis, Investigation, Methodology, Visualization, Writing - review & editing, **Samuel**
1014 **Chaffron:** Formal analysis, Investigation, Methodology, Visualization, Writing - review &
1015 editing, **Valérie Barbe:** Formal analysis, Visualization, Writing - review & editing, **Fabien**
1016 **Lombard:** Conceptualization, Funding acquisition, Investigation, Writing - review & editing,
1017 **Pedrotti Maria-Luiza:** Conceptualization, Funding acquisition, Project administration,
1018 Investigation, Writing - review & editing, **Gabriel Gorsky:** Conceptualization, Funding
1019 acquisition, Project administration, Investigation, Writing - review & editing, **Alexandra ter**
1020 **Halle:** Visualization, Writing - review & editing, **Stephane Bruzaud:** Visualization, Writing -
1021 review & editing, **Mikaël Kedzierski:** Formal analysis, Methodology, Visualization, Writing -
1022 review & editing, **Jean-François Ghiglione:** Conceptualization, Funding acquisition,
1023 Investigation, Methodology, Project administration, Resources, Supervision, Visualization,
1024 Writing - original draft, review & editing.

1025 **-Funding:** This work was supported by the European Union's Horizon 2020 research and
1026 innovation project AtlantECO under grant agreement No 862923. This work was part of the
1027 Ph.D thesis of J. Jacquin supported by research allocation from the French Ministry of Research
1028 (MENRT).

1029 **-Competing Interests:** The authors have no relevant financial or nonfinancial interests
1030 to disclose.

1031 **-Availability of data and materials:** The datasets and materials used and/or analyzed

1032 in the current study are available upon reasonable request.

1033 **Supplementary Text, Tables and Figures**

1034 **1. Supplementary Table 1.** Analysis of similarities test (ANOSIM, R and p-values) to evaluate if
 1035 differences of bacterial community structure were significantly related to different locations (Pacific vs.
 1036 Mediterranean) and type (FL, PA, PMD).

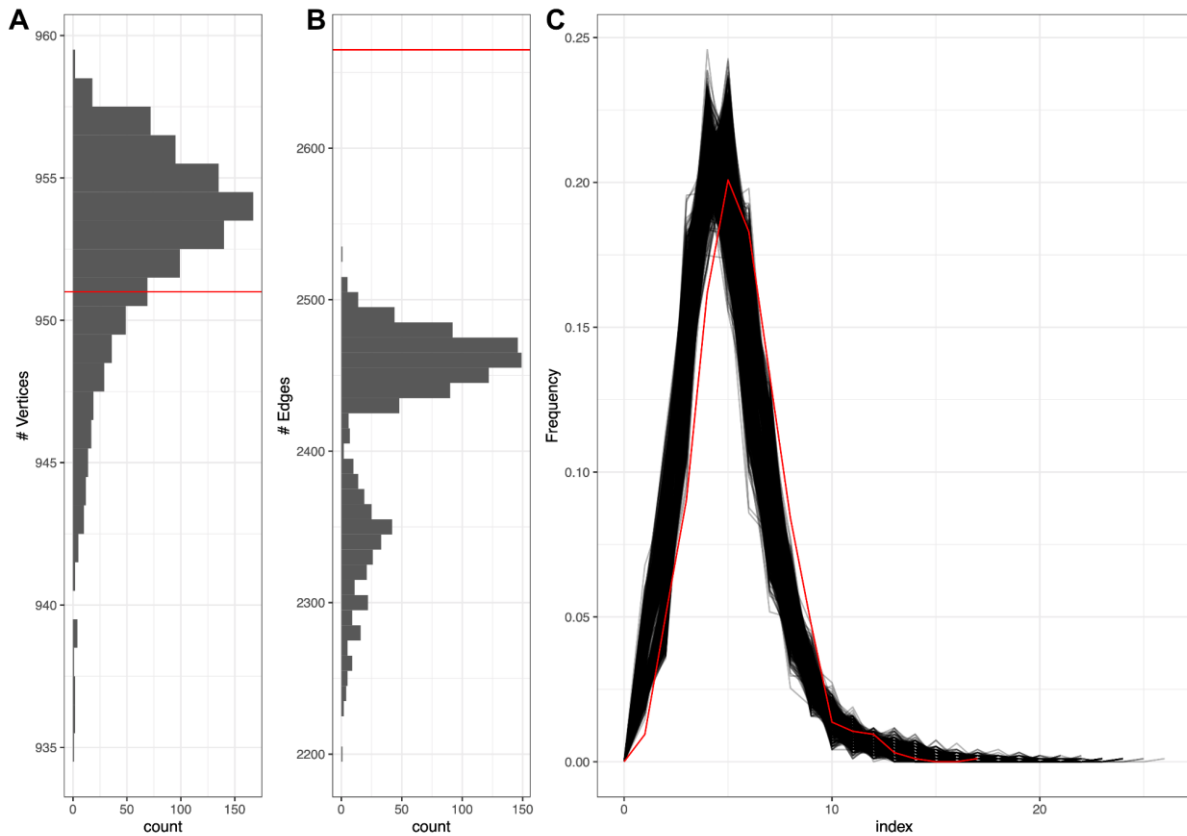
Location_1	Type_1	Location_2	Type_2	ANOSIM	p-value
Pacific	FL	Mediterranean	FL	0.4066	0.004
Pacific	FL	Pacific	PA	0.7191	0.001
Pacific	FL	Mediterranean	PA	0.6211	0.001
Pacific	FL	Pacific	PMD	0.9933	0.001
Pacific	FL	Mediterranean	PMD	0.8165	0.001
Mediterranean	FL	Pacific	PA	0.7427	0.001
Mediterranean	FL	Mediterranean	PA	0.5333	0.001
Mediterranean	FL	Pacific	PMD	0.9544	0.001
Mediterranean	FL	Mediterranean	PMD	0.7136	0.001
Pacific	PA	Mediterranean	PA	0.4253	0.001
Pacific	PA	Pacific	PMD	0.8711	0.001
Pacific	PA	Mediterranean	PMD	0.6720	0.001
Mediterranean	PA	Pacific	PMD	0.9178	0.001
Mediterranean	PA	Mediterranean	PMD	0.6204	0.001
Pacific	PMD	Mediterranean	PMD	0.4761	0.001

1037

1038 **2. Supplementary text and Supplementary Figure 1**

1039 **Biases due to sample imbalance in Network Construction**

1040 To check biases due to imbalanced sampling between the Mediterranean Sea (n=114) and the
 1041 Pacific Ocean (n=104), we reconstructed 1000 networks by randomly selecting 75 Pacific
 1042 samples and compared them with the network obtained using the entire PMD dataset (**Figure**
 1043 **1**). We observed that using the entire dataset inferred approximately the same number of nodes
 1044 (**Figure 1 A**) while ~10% more associations (**Figure 1 B**). These extra associations did not
 1045 impact the network structure measured by its degree distribution (**Figure 1 C**), so we concluded
 1046 that using the entire PMD dataset network allowed us to gather more information without
 1047 affecting ecological interpretations. Therefore, the network derived using the entire dataset was
 1048 used in the analyses.



1049

1050 **Supplemental Figure 1.** Simulation analysis for network reconstruction. The red line in panels A, B and
 1051 C shows the value obtained for the network containing all the samples. A) Number of vertices (i.e.,
 1052 nodes) in the 1000 network dataset. B) Number of edges (i.e., associations) in the 1000 network dataset
 1053 and C) Degree distribution in the 1000 networks

1054 **2. Relative abundance of modules in samples and co-occurrences between modules**

1055

1056 **Supplementary Table 1.** Wilcoxon tests on Mediterranean / Pacific prevalence based on CLR values on
 1057 PMD Samples. Q.value correction using FDR.

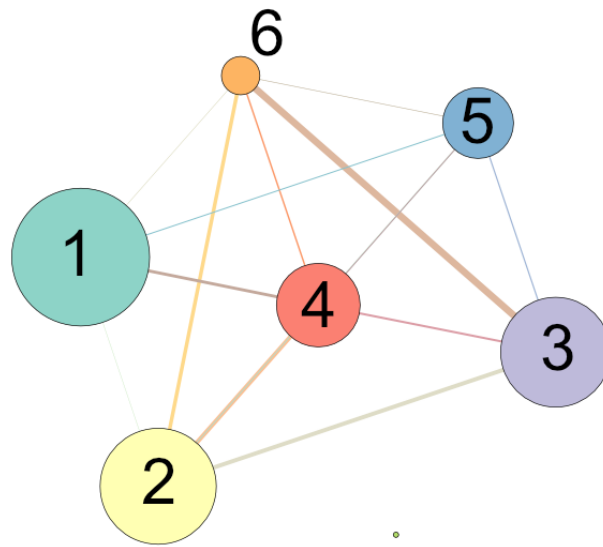
1058

module	p.value	q.value
1	4.44E-17	3.11E-16
2	7.03E-15	2.46E-14
3	2.71E-04	6.33E-04
4	9.69E-01	9.69E-01
5	7.60E-01	8.87E-01
6	9.80E-03	1.71E-02
7	2.44E-01	3.41E-01

1059

1060

1061



1062

1063 **Supplemental Figure 2.** Links between modules. The entire network was contracted into modules and represented
1064 as a graph. Node size is proportional to the number of OTUs in each module, whereas edge size between nodes is
1065 proportional to the number of co-occurrences between OTUs in each module

1066

1067 **3. Predictive metagenomic analysis**

1068 **Supplemental Figure 3: Relative abundance of L3 pathways within L2 and ocean-niche groups.**

